

Closed-Form CRLBs for CFO and Phase Estimation From Turbo-Coded Square-QAM-Modulated Transmissions

Fauzi Bellili, Achref Methenni, and Sofiène Affes, *Senior Member, IEEE*

Abstract—In this paper, we consider the problem of joint phase and carrier frequency offset (CFO) estimation for turbo-coded systems. We derive for the first time the closed-form expressions for the exact Cramér-Rao lower bounds (CRLBs) of these estimators over turbo-coded square-QAM-modulated single- or multi-carrier transmissions. In the latter case, the derived bounds remain valid in the general case of adaptive modulation and coding (AMC) where the coding rate and modulation order vary from one subcarrier to another depending on the corresponding channel quality information (CQI). In particular, we introduce a new recursive process that enables the construction of arbitrary Gray-coded square-QAM constellations. Some hidden properties of such constellations will be revealed, owing to this recursive process, and carefully handled to decompose the system's likelihood function (LF) into the sum of two analogous terms. This decomposition makes it possible to carry out *analytically* all the statistical expectations involved in the Fisher information matrix (FIM). The new analytical CRLB expressions corroborate the previous attempts to evaluate the underlying bounds *empirically*. In the low-to-medium signal-to-noise ratio (SNR) region, the CRLB for code-aided (CA) estimation lies between the bounds for completely blind [non-data-aided (NDA)] and completely data-aided (DA) estimation schemes, thereby highlighting the effect of the coding gain. Most interestingly, in contrast to the NDA case, the CA CRLBs start to decay rapidly and reach the DA bounds at relatively small SNR thresholds. It will also be shown that contrary to the CRLB of the phase shift, the CRLB of the CFO improves in a multi-carrier system as compared to its counterpart in a single-carrier system. The derived bounds are also valid for LDPC-coded systems and they can be evaluated in the same way when the latter are decoded using the turbo principal.

Index Terms—Carrier phase, carrier frequency offset (CFO), Cramér-Rao lower bound (CRLB), turbo codes, code-aided, extrinsic information, Gray mapping, square quadrature amplitude modulation (QAM) modulations, LDPC, square quadrature amplitude modulation (QAM), multi-carrier, adaptive modulation and coding (AMC).

Manuscript received January 18, 2014; revised June 8, 2014 and October 4, 2014; accepted December 7, 2014. Date of publication January 6, 2015; date of current version May 7, 2015. The associate editor coordinating the review of this paper and approving it for publication was Z. Wang. This work was supported by the Discovery Grants Program of NSERC and a Discovery Accelerator Supplement (DAS) Award.

The authors are with Energy, Materials and Telecommunications Center of Institut National de la Recherche Scientifique (INRS-EMT), Montreal, QC H5A 1K6, Canada (e-mail: bellili@emt.inrs.ca; methenni@emt.inrs.ca; affes@emt.inrs.ca).

Color versions of one or more of the figures in this paper are available online at <http://ieeexplore.ieee.org>.

Digital Object Identifier 10.1109/TWC.2014.2387855

I. INTRODUCTION

CURRENT and next-generation wireless communication systems are called upon to provide high quality of service, while satisfying the ever-increasing demand in high data rates. To meet these requirements, the use of powerful error-correcting codes in conjunction with high spectral efficiency modulations such as high-order quadrature amplitude modulations (QAMs) is advocated. These modulations are, indeed, a key feature of current and future wireless communication standards such as 4G long-term evolution (LTE), LTE-advanced (LTE-A) and beyond (LTE-B) [1]. On the other hand, turbo codes [2], [3] have gained considerable attention over the last two decades [4]. Owing to their impressive ability to operate in the near-Shannon limit (even at very low SNRs), they have also been adopted for 4G mobile communication systems such as Mobile WiMAX (IEEE 802.16e) [5] and 3GPP-LTE [6], [7].

Yet, turbo codes are known to be very sensitive to synchronization errors. That is, even small mismatches between the transmitter's and receiver's local oscillators (CFO) and/or small phase shifts (introduced by the wireless channel) can lead to severe performance degradations. One of the obvious solutions to this problem consists in using turbo codes in conjunction with a coherent detection scheme. In plain English, the carrier phase shift and the CFO are estimated and compensated for before proceeding to data decoding. As such, the synchronization parameters are estimated directly from the received samples at the output of the matched filter. In this case, two estimation schemes can be envisaged i) NDA estimation with no *a priori* knowledge about the transmitted symbols or ii) DA estimation using perfectly known pilot symbols (training sequence). In both cases, however, accurate synchronization is quite challenging for turbo-coded systems since they are primarily intended to operate at low signal-to-noise ratios (SNRs). Indeed, in such adverse SNR conditions, practical¹ NDA and DA techniques may result in high estimation errors; affecting thereby the overall system performance.

To circumvent this problem and to properly synchronize turbo-coded systems at low SNR, two different and more

¹In principle, the performance of NDA or DA techniques can be improved indefinitely by increasing the observation window size or inserting more pilot symbols, respectively. However, the observation window size in NDA estimation is limited by many practical constraints such as the delay tolerated by the system and/or its ability to operate properly beyond the coherence time. Furthermore, using long preambles in DA estimation impinges directly on the whole throughput of the system and decreases its effective transmission rate.

elaborate approaches were adopted in the open literature. In both approaches, the estimation task is assisted by the decoder. Therefore, we will refer to it in this paper as *code-aware* or *code-assisted* (CA) estimation, as opposed to non-code-aided (NCA) estimation (i.e., NDA scenario). The first approach consists in modifying the structure of the classical soft-input-soft-output (SISO) decoder and embedding in it the estimation task. As one example in [8], the forward and backward recursions have been modified to perform the decoding and estimation tasks jointly (see also [9]). In the second approach, however, the structure of the SISO decoder is not altered and it is usually referred to as *turbo synchronization*. Rather, the estimation process relies directly on the use of the soft information (either the *a posteriori* probabilities or the *extrinsic* information) provided by the turbo receiver at each decoding iteration (see [8], [10]–[21] and references therein). For instance, using the *a posteriori* probabilities and the *extrinsic* information, the carrier phase and the CFO are estimated jointly with turbo decoding in [10] and [11], respectively. A more recent work dealing with doubly-selective channels and CFO CA estimation from turbo-coded QAM-modulated signals in OFDM systems was introduced in [12].

To evaluate the achievable performance limit in the estimation of the synchronization parameters, an absolute benchmark must be evaluated. The Cramér-Rao lower bound (CRLB), a well known fundamental bound [22], meets this requirement since it sets the minimum achievable variance for any unbiased estimator. Most interestingly and unlike other loose bounds, the *stochastic* CRLB (unknown and random transmitted symbols) is known to be achieved asymptotically by the stochastic maximum likelihood (ML) estimator. Yet, even under uncoded transmissions, the complex structure of the LF makes it extremely hard, if not impossible, to derive analytical expressions for this bound, especially for high-order modulations. Therefore, it is often evaluated empirically (in both NCA and CA estimations). Indeed, the stochastic CRLBs for the carrier phase and CFO NDA estimation were first evaluated empirically for the uncoded PSK- and symmetric-QAM-modulated signals in [23]. It was only recently, though, that their closed-form expressions have been established for BPSK/QPSK transmissions in [25] and for general square-QAM-modulated signals in [26], but still in the traditional NCA scenario.² In coded transmissions, however, the LF becomes even more complicated and developing such bounds in closed form is trivially more difficult. Thus, exhaustive Monte-Carlo simulations have been recently used by Noels *et al.* in [33], [36] to evaluate *empirically* the CRLBs for CA estimates of the carrier phase and CFO parameters from turbo-coded linearly-modulated signals. However, although much needed, their closed-form expressions have not been yet reported in the open literature. Motivated by these facts, we derive for the very first time the analytical expressions for the considered CRLBs in CA estimation from any

turbo-coded square-QAM-modulated signal for both single- or multi-carrier transmissions and show that they corroborate the aforementioned attempts to evaluate these bounds *empirically* in the single-carrier case only [33], [36]. The derived bounds are also valid for LDPC-coded systems and they can be evaluated when the latter are decoded using the turbo principal since in this case the MAP SISO decoder outputs the *extrinsic* information which is the only needed quantity to evaluate the newly derived CRLBs.

The rest of this paper is structured as follows. In Section II, we present the system model. In Section III, we introduce the recursive process that allows the construction of any square-QAM Gray-coded constellation and relate the symbols' *a priori* probabilities (APPs) to the bits' log-likelihood ratios (LLRs). In Section IV, we factorize the probability density function (pdf) of each received sample into two analogous terms. In Section V, we derive the different FIM elements and the analytical expressions for the considered CRLBs. In Section VI, we extend these expressions to multi-carrier transmissions over multi-path channels. In Section VII, we discuss the simulation results of the new bounds and, finally, draw out some concluding remarks in Section VIII.

In the sequel, some of the common notations will be used. In fact, vectors and matrices are represented in lower- and upper-case bold fonts, respectively. Moreover, $\{\cdot\}^T$ and $\{\cdot\}^H$ denote the transpose and the Hermitian (transpose conjugate) operators, respectively. The operators $\Re\{\cdot\}$ and $\Im\{\cdot\}$ return, respectively, the real and imaginary parts of any complex number. The operators $\{\cdot\}^*$ and $|\cdot|$ return its conjugate and its amplitude, respectively, and j is the pure complex number that verifies $j^2 = -1$. We will also denote the probability mass function (PMF) for discrete random variables by $Pr[\cdot]$ and the pdf for continuous random variables by $p[\cdot]$. The statistical expectation with respect to any random variable is denoted as $E\{\cdot\}$.

II. SYSTEM MODEL

Consider a *flat-fading*³ *single-carrier* turbo-coded system where a binary sequence of information bits is fed into a turbo encoder of rate R . The encoder consists of two identical recursive and systematic convolutional codes (RSCs) with generator polynomials $[g_1, g_2]$. The two RSCs are concatenated in parallel via an interleaver of size L . The coded bits are then fed into a puncturer which selects an appropriate combination of the parity bits, from both encoders, to achieve the desired code rate R . The obtained code bits (systematic and parity bits) are then interleaved, with an outer interleaver, and mapped onto a given Gray-coded constellation. The obtained symbols are then transmitted over the wireless channel and the corresponding received signal is sampled at the output of the matched filter. In this paper, we make the following basic assumptions:

- 1) Perfect time synchronization.

²Note here that closed-form CRLBs for NDA estimation of other channel parameters in higher-order square-QAM transmissions have been derived analytically only recently as well. For instance, the reader is referred to [27], [28] for SNR estimation, [29] for DOA estimation, and [30], [31] for timing recovery, respectively.

³It should be mentioned, however, that OFDM systems transform a (multipath) frequency-selective channel in the time domain into a frequency-flat (i.e., narrowband) channel over each subcarrier as modeled by (2) [34], [35]. For these reasons and for the sake of clarity, the detailed derivations will be conducted for a single-carrier *flat-fading* channel and extensions to multicarrier channels will be discussed in Section VI.

- 2) The shaping pulse, $p(t)$, verifies the first Nyquist criterion, i.e., the convolution:

$$g(x) = \int_{-\infty}^{+\infty} p(x)p(t+x)dx, \quad (1)$$

satisfies the condition $g(nT) = 0 \forall n \neq 0$ where T is the symbol period.

- 3) The frequency offset is very small compared to the signal bandwidth.

Owing to these three assumptions, the base-band received samples in the presence of phase and frequency distortions are modeled⁴ as follows [37]:

$$y(k) = Sx(k)e^{j(2\pi kv + \phi)} + w(k), \quad (2)$$

$$k = k_0, k_0 + 1, \dots, k_0 + K - 1,$$

where K is the total number of recorded data and k_0 refers to the time instant of the first observed sample. The channel coefficient, S , is assumed to be slowly-time varying and, therefore, constant over the observation window. In this paper, it is treated as an unknown but *deterministic* parameter. Of course, it might be random in practice. And if its statistical properties are known beforehand, they can be used to improve the estimation performance (i.e., lower CRLB). However, even in the easiest case of Rayleigh fading, the upcoming derivations become extremely cumbersome and the considered CRLBs cannot be derived in closed form. For these reasons, the *a priori* knowledge about the statistics of the channel can be disregarded during the estimation process by assuming it unknown but *deterministic*.

At each sampling index k , $x(k)$ is an unknown transmitted symbol and $y(k)$ is the corresponding received sample. The transmitted symbols $\{x(k)\}_k$ are drawn from any M -ary Gray-coded square-QAM constellation whose alphabet is denoted as $C_p = \{c_0, c_1, \dots, c_{M-1}\}$. By *square* QAM we mean $M = 2^{2p}$ (i.e., QPSK, 16-QAM, 64-QAM, etc...). The noise components, $\{w(k)\}_k$, are modeled by zero-mean circular complex Gaussian random variables with independent real and imaginary parts (each of variance σ^2). For more convenience, the unknown phase and frequency offsets (respectively, ϕ and v) are stacked into a single parameter vector $\alpha = [\phi \ v]^T$. They are to be estimated from all the received samples gathered in the observation vector $y = [y(k_0), y(k_0 + 1), \dots, y(k_0 + K - 1)]^T$. Without loss of generality (w.l.o.g), we will also assume that the energy of the transmitted symbols is normalized to one⁵ (i.e., $E\{|x(k)|^2\} = 1$) so that the average SNR of the system is given by $\rho = E\{S^2|x(k)|^2\}/2\sigma^2 = S^2/2\sigma^2$.

Now, suppose that we are able to produce an unbiased estimate, $\hat{\alpha}$, of the parameter vector α , from the received vector y . Then, the CRLB is a practical lower bound [22] that

verifies⁶ the inequality $E\{[\hat{\alpha} - \alpha][\hat{\alpha} - \alpha]^T\} \succeq \text{CRLB}(\alpha)$. It is given by:

$$\text{CRLB}(\alpha) = I^{-1}(\alpha), \quad (3)$$

where $I(\alpha)$ is the Fisher information matrix (FIM) whose entries are expressed:

$$[I(\alpha)]_{i,l} = -E\left\{\frac{\partial^2 L(y; \alpha)}{\partial \alpha_i \partial \alpha_l}\right\} \quad i, l = 1, 2. \quad (4)$$

In (4), $\{\alpha_i\}_{i=1,2}$ are the elements of the unknown parameter vector α and $L(y; \alpha) \triangleq \ln(p[y; \alpha])$ is the log-likelihood function (LLF) of the system ($p[y; \alpha]$ is the pdf of y parameterized by α). As seen from (4), the first step in deriving the tackled bounds is to find an explicit expression for the LLF or equivalently the pdf $p[y; \alpha]$. To that end, the APPs, $Pr[x(k) = c_m]$, of the transmitted symbols involved in (2) must be found.

At this stage, it is worth mentioning in NDA estimation, where no *a priori* information is available, that the transmitted symbols are usually assumed to be equally likely, i.e., $Pr[x(k) = c_m] = 1/M$ for $k = k_0, k_0 + 1, \dots, k_0 + K - 1$. In code-aided estimation, however, the actual APPs of the symbols must be used to enhance the estimation performance. Indeed, in the next section, we will express them in terms of the LLRs of the conveyed bits. In practice, the information about the LLRs is acquired from the output of the soft-input soft-output (SISO) decoder at the convergence of the BCJR algorithm [32].

III. DERIVATION OF THE SYMBOLS' APPS

Throughout this paper, we assume that the constellation is Gray coded. Each point of the alphabet, $\{c_m\}_{m=1}^M$, is mapped onto a unique sequence of $\log_2(M)$ bits denoted here as $\bar{b}_1^m \bar{b}_2^m \dots \bar{b}_l^m \dots \bar{b}_{\log_2(M)}^m$. For the sake of clarity, this mapping will be denoted as follows:⁷

$$c_m \longleftrightarrow \bar{b}_1^m \bar{b}_2^m \dots \bar{b}_l^m \dots \bar{b}_{\log_2(M)}^m. \quad (5)$$

The same notation is used to refer to the k^{th} bit sequence, $b_1^k b_2^k \dots b_l^k \dots b_{\log_2(M)}^k$, that is conveyed during the transmission of the k^{th} symbol $x(k)$, i.e., $x(k) \longleftrightarrow b_1^k b_2^k \dots b_l^k \dots b_{\log_2(M)}^k$. Then, due to the large-size interleaver, the coded bits can reasonably be assumed as statistically independent. This is a standard assumption in CA estimation practices (see [33]–[42] and references therein). Therefore, the *a priori* probability of each transmitted symbol, $x(k)$, factorizes into the elementary probabilities of its conveyed bits:

$$Pr[x(k) = c_m] = Pr\left[b_1^k = \bar{b}_1^m, b_2^k = \bar{b}_2^m, \dots, b_{\log_2(M)}^k = \bar{b}_{\log_2(M)}^m\right] \\ = \prod_{l=1}^{\log_2(M)} Pr\left[b_l^k = \bar{b}_l^m\right]. \quad (6)$$

⁶Note that $A \succeq B$ for any two square matrices A and B means that $A - B$ is positive semi-definite.

⁷To avoid any confusion between the bit sequence assigned to a given constellation symbol, c_m , and the (*data*) bit sequence that is conveyed whenever $x(k) = c_m$, we use the overbar in (5) in contrast to $x(k) \longleftrightarrow b_1^k b_2^k \dots b_l^k \dots b_{\log_2(M)}^k$. See (6) for more details.

⁴The detailed derivation of the discrete model (2) from the analog received signal can be found in [37, Chap. 2].

⁵If the transmit energy, P , is not unitary, it can be easily incorporated as an unknown scaling factor into the channel coefficient which becomes \sqrt{PS} instead of S in (2).

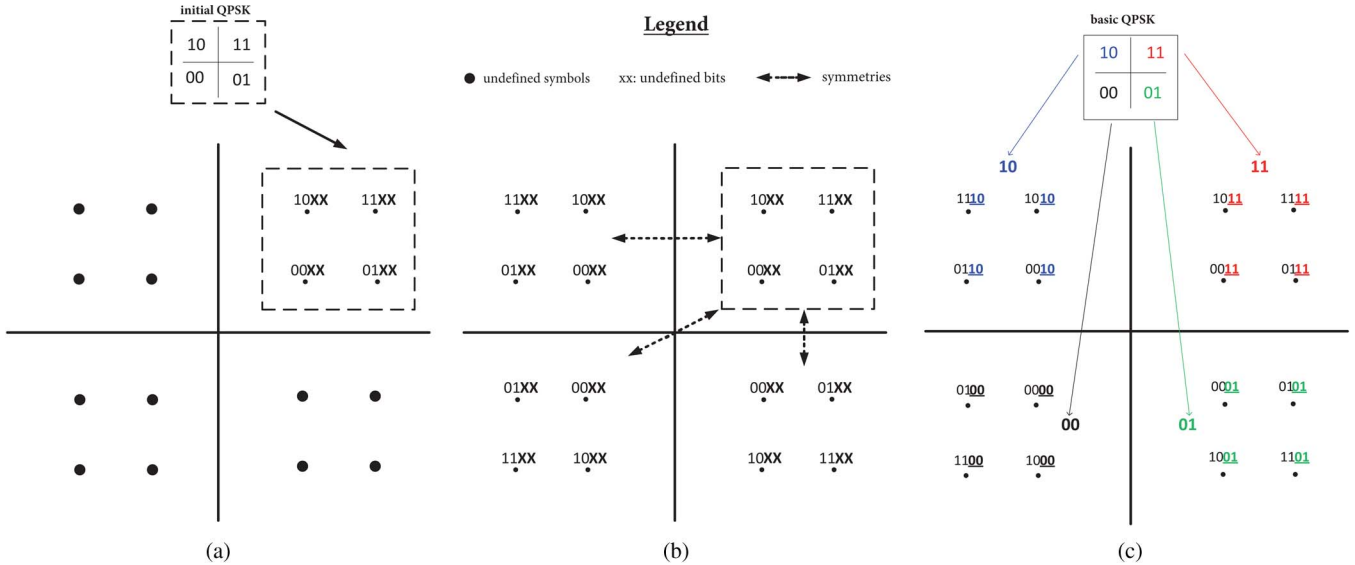


Fig. 1. Recursive construction of Gray-coded square-QAM constellations illustrated here from 4-QAM to 16-QAM.

We also define the LLR of the l^{th} coded bit, b_l^k , conveyed by the transmission of the symbol, $x(k)$, as follows:

$$L_l(k) \triangleq \ln \left(\frac{Pr[b_l^k = 1]}{Pr[b_l^k = 0]} \right). \quad (7)$$

Using (7) and the fact that $Pr[b_l^k = 0] + Pr[b_l^k = 1] = 1$, it can be easily shown that:

$$Pr[b_l^k = 1] = \frac{e^{L_l(k)}}{1 + e^{L_l(k)}} \text{ and } Pr[b_l^k = 0] = \frac{1}{1 + e^{L_l(k)}}. \quad (8)$$

For every c_m in C_p , if $x(k) = c_m$, then the two identities in (8) can be merged together to yield a generic expression for the elementary probabilities involved in (6) as follows:

$$Pr[b_l^k = \bar{b}_l^m] = \frac{1}{2 \cosh(L_l(k)/2)} e^{(\bar{b}_l^m - 1) \frac{L_l(k)}{2}}, \quad (9)$$

in which \bar{b}_l^m is either 0 or 1 depending on which of the symbols c_m is transmitted, at time instant k , and of course on the Gray mapping that is associated to the constellation in (5). Therefore, injecting (9) in (6) and recalling that $\log_2(M) = 2p$ for square-QAM constellations, the symbols' APPs develop into:

$$Pr[x(k) = c_m] = \underbrace{\left(\prod_{l=1}^{2p} \frac{1}{2 \cosh(L_l(k)/2)} \right)}_{\beta_k} \prod_{l=1}^{2p} e^{(\bar{b}_l^m - 1) \frac{L_l(k)}{2}}. \quad (10)$$

Next, we describe a simple process that allows—as will be shown later—the construction of arbitrary Gray-coded square-QAM constellations. Owing to this recursive process, some hidden properties of such constellations will be revealed and carefully handled to rewrite the APPs in (10) in a more insightful form that allows the LF factorization in the next section.

In fact, using any *basic* Gray-coded QPSK and starting from any given Gray-coded $2^{2(p-1)}$ -QAM, it is possible to build another Gray-coded 2^{2p} -QAM as follows:

- *step 1*: build the top-right quadrant of the desired 2^{2p} -QAM from all the points⁸ of the available $2^{2(p-1)}$ -QAM. As such, all the points of the new quadrant are still missing two out of the $2p$ bits they must represent. This is simply because they were cloned from the given $2^{2(p-1)}$ -QAM whose points actually represent $2p - 2$ bits only. For the sake of clarity and again w.l.o.g, we will assume that these two missing bits always occupy the two least significant positions in each point of the new quadrant.
- *step 2*: build the remaining empty quadrants (bottom-right, top-left and bottom-left) of the desired 2^{2p} -QAM by symmetries with respect to the x -axis, the y -axis, and the center point, respectively. In light of “*step 1*”, all the points of the desired constellation are inherently missing two bits each.
- *step 3*: copy the two bits of each quadrant in the basic Gray-coded QPSK constellation to all the points that belong to the same quadrant in the incomplete 2^{2p} -QAM constellation obtained in “*step 2*”.

One example that clearly depicts these three steps is shown in Fig. 1 (illustrated here in initial transition from 4-QAM to 16-QAM). The two missing bits in “*step 1*” and “*step 2*” are denoted as “ $\times \times$ ” in Fig. 1(a) and 1(b). They are added in “*step 3*” and highlighted in four different colors; one for each quadrant. We show in Appendix A that this recursive process yields indeed Gray-coded constellations.

Furthermore, by closely inspecting Fig. 1, it can be seen that to obtain all the possible Gray-coded 16-QAM constellations, one can simply: *i*) start from any other *initial* Gray-coded QPSK, *ii*) use other *basic* QPSK constellations, and *iii*) let the

⁸The same points' layout in the original $2^{2(p-1)}$ -QAM constellation is used, i.e., the constellation is placed as is in the new quadrant.

two missing bits in “step 1” occupy any two positions, i.e., neither being necessarily consecutive nor being the two LSBs. To obtain all the possible 64-QAM Gray-coded constellations, one can simply start from each of the obtained 16-QAMs and consider *ii*) and *iii*) stated above. In this way, the new recursive process enables the easy construction of any square-QAM Gray-coded constellation. For the sake of clarity and conciseness, however, and again w.l.o.g, we will from now on consider the QPSK constellation depicted in Fig. 1(c) as the *basic* one and will actually use it in both the *initial* and all subsequent construction iterations required for a given modulation order. For the same reasons, we will also assume that the two missing bits in “step 1” are always the two LSBs.

Now, recalling that C_p denotes the whole alphabet of the obtained 2^{2p} -QAM Gray-coded constellation, we further denote its top-right quadrant by \tilde{C}_p . As such, each point $c_m \in C_p$ belongs to a set of four symmetrical points $\{\tilde{c}_m, \tilde{c}_m^*, -\tilde{c}_m, -\tilde{c}_m^*\}$ for some \tilde{c}_m in \tilde{C}_p . Moreover, due to symmetries of “step 2,” these four symmetrical points share the same $2p - 2$ most significant bits (MSBs), $\bar{b}_1^m \bar{b}_2^m \bar{b}_3^m \dots \bar{b}_{2p-3}^m \bar{b}_{2p-2}^m$.

Consequently, if we consider these $2(p - 1)$ MSBs alone and we define the quantity:

$$\mu_{k,p}(c_m) \triangleq \prod_{l=1}^{2p-2} e^{(2\bar{b}_l^m - 1) \frac{L_l(k)}{2}}, \quad \forall c_m \in C_p, \quad (11)$$

it follows from (10) that:

$$Pr[x(k) = c_m] = \beta_k \mu_{k,p}(c_m) e^{(2\bar{b}_{2p-1}^m - 1) \frac{L_{2p-1}(k)}{2}} e^{(2\bar{b}_{2p}^m - 1) \frac{L_{2p}(k)}{2}} \quad (12)$$

with:

$$\mu_{k,p}(\tilde{c}_m) = \mu_{k,p}(-\tilde{c}_m) = \mu_{k,p}(\tilde{c}_m^*) = \mu_{k,p}(-\tilde{c}_m^*). \quad (13)$$

It is worth mentioning here that—as seen from the right-hand side of (11)— $\mu_{k,p}(c_m)$ is not defined for $p = 1$, i.e., for QPSK constellations. We extend its definition for the latter simply by taking $\mu_{k,1}(c_m) = 1 \forall c_m \in C_1$. It will be seen later that this choice is consistent with all the derivations. Now, the two bits $\bar{b}_{2p-1}^m \bar{b}_{2p}^m$ involved in the two remaining exponentials in (12) are exactly the same for all the symbols that belong to the same quadrant in the obtained 2^{2p} -QAM constellation (recall that they are added in “step 3”). Typically, by considering the *basic* QPSK depicted in Fig. 1(c), they are given by:

$$\bar{b}_{2p-1}^m \bar{b}_{2p}^m = \begin{cases} 11 & \forall \tilde{c}_m \in \tilde{C}_p \\ 00 & \forall -\tilde{c}_m \in -\tilde{C}_p. \end{cases} \quad (14)$$

$$\bar{b}_{2p-1}^m \bar{b}_{2p}^m = \begin{cases} 01 & \forall \tilde{c}_m^* \in \tilde{C}_p \\ 10 & \forall -\tilde{c}_m^* \in -\tilde{C}_p. \end{cases} \quad (15)$$

Of course, these intermediate results change according to the specific choice of the *basic* QPSK constellation involved in “step 3.” Consequently, one might wonder how the final results could still stand valid for all possible Gray-mapping schemes of the underlying 2^{2p} -QAM constellation. Actually, in this paper, \tilde{C}_p is willingly defined as the top-right quadrant simply because the two bits “11” are placed in the top-right quadrant of the considered *basic* QPSK constellation. Therefore, the same

upcoming derivations can be conducted by defining \tilde{C}_p to be the quadrant that reflects the bits “11” in any other choice of the *basic* QPSK constellation. By using (14) and (15) in (12) and recalling (13), it follows that:

$$Pr[x(k) = \tilde{c}_m] = \beta_k \mu_{k,p}(\tilde{c}_m) e^{-\frac{L_{2p-1}(k)}{2}} e^{\frac{L_{2p}(k)}{2}}, \quad (16)$$

$$Pr[x(k) = \tilde{c}_m^*] = \beta_k \mu_{k,p}(\tilde{c}_m) e^{-\frac{L_{2p-1}(k)}{2}} e^{-\frac{L_{2p}(k)}{2}}, \quad (17)$$

$$Pr[x(k) = -\tilde{c}_m] = \beta_k \mu_{k,p}(\tilde{c}_m) e^{-\frac{L_{2p-1}(k)}{2}} e^{-\frac{L_{2p}(k)}{2}}, \quad (18)$$

$$Pr[x(k) = -\tilde{c}_m^*] = \beta_k \mu_{k,p}(\tilde{c}_m) e^{\frac{L_{2p-1}(k)}{2}} e^{-\frac{L_{2p}(k)}{2}}. \quad (19)$$

By scanning the top-right quadrant, \tilde{C}_p , these four equations (defined for every \tilde{c}_m and its three symmetrical points in the other quadrants) form the complete set of APPs for each symbol $x(k)$. By doing so, every four symmetrical points ($\tilde{c}_m, \tilde{c}_m^*, -\tilde{c}_m$, and $-\tilde{c}_m^*$) exhibit a common multiplicative factor $\beta_k \mu_{k,p}(\tilde{c}_m)$. This interesting property will prove very useful in factorizing the elementary pdfs, $p[y(k), \alpha]$, in the next section.

Note here that all the manipulations used to obtain the expressions for the APPs in (16)–(19) are intrinsic to the Gray-coded constellation only and do not need any assumption about the specific encoder at the transmitter. Therefore, (16)–(19) and the CA CRLBs derived in this paper are actually valid for coded transmissions in general. In the evaluation of the CA CRLBs, however, as will be seen later, one needs accurate estimates for the bits’ LLRs. Such estimates are obtained from the output of the SISO decoder in turbo-coded or LDPC-coded systems jointly used with turbo processing [38], [39].

IV. FACTORIZATION OF $p[y(k); \alpha]$

Recall from (4) that an explicit expression for the global LLF of the system, $L(y; \alpha) \triangleq \ln(p[y; \alpha])$, must be found before being able to derive the analytical CRLBs. Actually, since the coded bits are assumed to be statistically independent (due to the large-size interleaver), the transmitted symbols (which are simply some *soft* representations for different blocks of these bits) are also independent thereby leading to:

$$p[y; \alpha] = \prod_{k=k_0}^{k_0+K-1} p[y(k); \alpha]. \quad (20)$$

Consequently, the global LLF breaks down to the sum of the elementary LLFs (pertaining to each received sample), i.e., $L(y; \alpha) = \sum_{k=k_0}^{k_0+K-1} \ln(p[y(k); \alpha])$. In this section, we will show for any square-QAM constellation that the pdf of each received sample, $p[y(k); \alpha]$, is further factorized into the product of two analogous terms linearizing thereby the elementary LLFs. Then, owing to the apparent symmetries between the two analogous terms, it is possible to derive the analytical expressions for the considered bounds in Section V.

To start with, it can be seen from (2) that the pdf of each received sample, $y(k)$, parameterized by the unknown parameter vector, α , is given by:

$$p[y(k); \alpha] = \sum_{c_m \in C_p} Pr[x(k) = c_m] p[y(k); \alpha | x(k) = c_m] \\ = \frac{1}{2\pi\sigma^2} \sum_{c_m \in C_p} Pr[x(k) = c_m] \exp\left\{-\frac{|y(k) - S_{\phi, v} c_m|^2}{2\sigma^2}\right\}, \quad (21)$$

in which we use the shorthand notation $S_{\phi, v} \triangleq S e^{j(2\pi k v + \phi)}$.

Then, denoting the inphase (I) and quadrature (Q) components of the received sample, respectively, as $I(k) \triangleq \Re\{y(k)\}$ and $Q(k) \triangleq \Im\{y(k)\}$, it can be shown that in presence of general M -ary QAM-modulated signals, the pdf in (21) is rewritten as follows:

$$p[y(k); \alpha] = \frac{1}{2\pi\sigma^2} \exp\left\{-\frac{I(k)^2 + Q(k)^2}{2\sigma^2}\right\} D_\alpha(k), \quad (22)$$

in which the term $D_\alpha(k)$ is defined as:

$$D_\alpha(k) \triangleq \sum_{c_m \in C_p} P[x(k) = c_m] \\ \times \exp\left\{-\frac{S^2 |c_m|^2}{2\sigma^2}\right\} \exp\left\{\frac{\Re\{c_m y(k)^* S_{\phi, v}\}}{\sigma^2}\right\}, \quad (23)$$

In the sequel, we will further manipulate $D_\alpha(k)$ by exploiting other hidden properties of the Gray-coding mechanism which are demystified through our recursive construction process introduced in Section III (see Fig. 1). Actually, by focusing on square-QAM constellations (i.e., $M = 2^{2p}$ for any $p \geq 1$), it can be seen that their alphabet is expressed in the I/Q plane as $C_p = \{\pm(2i-1)d_p \pm j(2n-1)d_p\}_{i,n=1,2,\dots,2^{p-1}}$, where $2d_p$ is the intersymbol distance. Further, since the constellation energy is normalized to one, we have $\frac{1}{2^{2p}} \sum_{m=1}^{2^{2p}} |c_m|^2 = 1$ from which the expression of d_p is obtained as follows:

$$d_p = \frac{2^{p-1}}{\sqrt{2^p \sum_{m=1}^{2^{2p}-1} (2m-1)^2}}. \quad (24)$$

Then, by noticing that $C_p = \tilde{C}_p \cup (-\tilde{C}_p) \cup \tilde{C}_p^* \cup (-\tilde{C}_p^*)$, we show in Appendix B that (23) can be equivalently rewritten as a sum over \tilde{C}_p as follows:

$$D_\alpha(k) = 4\beta_k \sum_{\tilde{c}_m \in \tilde{C}_p} \mu_{k,p}(\tilde{c}_m) e^{-\rho|\tilde{c}_m|^2} \\ \times \cosh\left(\frac{S \Re\{\tilde{c}_m\} u(k)}{\sigma^2} + \frac{L_{2p}(k)}{2}\right) \\ \times \cosh\left(\frac{S \Im\{\tilde{c}_m\} v(k)}{\sigma^2} - \frac{L_{2p-1}(k)}{2}\right). \quad (25)$$

in which $u(k) \triangleq \Re\{y^*(k) e^{j(2\pi k v + \phi)}\}$ and $v(k) \triangleq \Im\{y^*(k) e^{j(2\pi k v + \phi)}\}$ are given by:

$$u(k) = I(k) \cos(2\pi k v + \phi) + Q(k) \sin(2\pi k v + \phi), \quad (26)$$

$$v(k) = I(k) \sin(2\pi k v + \phi) - Q(k) \cos(2\pi k v + \phi). \quad (27)$$

Using the fact that $\tilde{C}_p = \{(2i-1)d_p + j(2n-1)d_p\}_{i,n=1}^{2^{p-1}}$, one can replace the single sum over $\tilde{c}_m \in \tilde{C}_p$ in (25) by a double sum over the two counters i and n after replacing \tilde{c}_m by $(2i-1)d_p + j(2n-1)d_p$ [of course, $\Re\{\tilde{c}_m\} = (2i-1)d_p$ and $\Im\{\tilde{c}_m\} = (2n-1)d_p$]. Therefore, if we are able to factorize $\mu_{k,p}(\tilde{c}_m)$ as the product of two terms, one depending on i only and the other on n only, then $D_\alpha(k)$ will be factorized as well by splitting the two sums (over i and n). To do so, notice from (11) that the two LSBs, $\bar{b}_{2^{p-1}}^m$ and $\bar{b}_{2^p}^m$, are not involved in the expression of $\mu_{k,p}(\tilde{c}_m)$ and hence they will be represented by “ $\times \times$ ” in (5), i.e.:

$$\tilde{c}_m \longleftrightarrow \underbrace{\bar{b}_1^m \bar{b}_2^m \cdots \bar{b}_l^m \cdots \bar{b}_{2^{p-5}}^m \bar{b}_{2^{p-4}}^m \bar{b}_{2^{p-3}}^m \bar{b}_{2^{p-2}}^m}_{\bar{b}_p^m} \times \times. \quad (28)$$

In addition, as highlighted in (28) and for ease of notation, we will refer to the first $2p-4$ MSBs by \bar{b}_p^m , i.e., $\bar{b}_p^m \triangleq \bar{b}_1^m \bar{b}_2^m \cdots \bar{b}_l^m \cdots \bar{b}_{2^{p-5}}^m \bar{b}_{2^{p-4}}^m$. For more mathematical convenience that will become apparent shortly, we will rather use⁹ the superscript (i, n) instead of m in (28) since $\tilde{c}_m = (2i-1)d_p + j(2n-1)d_p$, i.e.:

$$\tilde{c}_m \longleftrightarrow \bar{b}_p^{(i,n)} \bar{b}_{2^{p-3}}^{(i,n)} \bar{b}_{2^{p-2}}^{(i,n)} \times \times. \quad (29)$$

Owing to this new notation, we re-illustrate in Fig. 2 the symbols of the top-right quadrant, \tilde{C}_p , of the obtained 2^{2p} -QAM constellation accordingly. In this figure, the bits $\bar{b}_{2^{p-2}}^{(i,n)}$ and $\bar{b}_{2^{p-3}}^{(i,n)}$ are being assigned their true values and highlighted in red color. Now, each point \tilde{c}_m in \tilde{C}_p with coordinates $([2i-1]d_p, [2n-1]d_p)$ in the Cartesian coordinate system (CCS) of the underlying 2^{2p} -QAM (defined by x - and y -axes in Fig. 2) is obtained from (coincides exactly with) a point $c_{m'}$ in the previous $2^{2(p-1)}$ -QAM. This is because the latter is placed as is in \tilde{C}_p (in “step 1”). Furthermore, $c_{m'}$ has its own coordinates, $([2i'-1]d_p, [2n'-1]d_p)$, in the CCS associated to the $2^{2(p-1)}$ -QAM constellation (defined by the x' - and y' -axes in Fig. 2). By closely inspecting the two CSSs in Fig. 2, it can be shown that $c_{m'}$ can be expressed in terms of either (i', n') or (i, n) as follows:

$$c_{m'} = (2i' - 1)d_p + j(2n' - 1)d_p \\ = (2i - 1 - 2^{p-1})d_p + j(2n - 1 - 2^{p-1})d_p. \quad (30)$$

This relationship will shortly serve an extremely useful lemma that finds an explicit expression for the two remaining bits in (29), $\bar{b}_{2^{p-2}}^{(i,n)}$ and $\bar{b}_{2^{p-3}}^{(i,n)}$, in terms of the coordinates of each symbol \tilde{c}_m in \tilde{C}_p . Note that the first $2p-2$ MSBs of each symbol $\tilde{c}_m \in \tilde{C}_p$ are exactly the whole bit sequence of the corresponding symbol $c_{m'}$ in the original $2^{2(p-1)}$ -QAM constellation. This means that we readily have $c_{m'} \longleftrightarrow \bar{b}_p^{(i,n)} \bar{b}_{2^{p-3}}^{(i,n)} \bar{b}_{2^{p-2}}^{(i,n)}$. Equivalently, denoting the top-right quadrant of the $2^{2(p-1)}$ -QAM constellation by \tilde{C}_{p-1} , the symbol $c_{m'}$ itself belongs to its own

⁹Normally, we should use (i_m, n_m) but, for ease of notation, we drop the index m and simply use (i, n) .

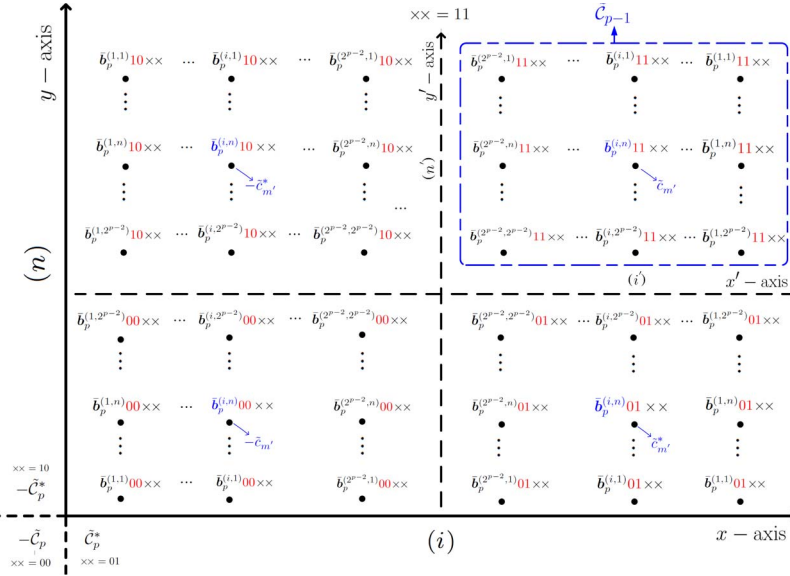


Fig. 2. General recursive construction of Gray-coded square-QAM constellations from $2^{2(p-1)}$ -QAM to 2^{2p} -QAM.

set of four symmetrical points, i.e., $c_{m'} \in \{\tilde{c}_{m'}, -\tilde{c}_{m'}, \tilde{c}_{m'}^*, -\tilde{c}_{m'}^*\}$ for some $\tilde{c}_{m'} \in \tilde{C}_{p-1}$, and are marked by four blue-colored arrows in Fig. 2. Recall also that the $2^{2(p-1)}$ -QAM constellation itself is obtained from another lower-order Gray-coded $2^{2(p-2)}$ -QAM, by applying the same recursive process. Then, owing to the three symmetries of “step 2”, it follows that $\tilde{c}_{m'}$, $-\tilde{c}_{m'}$, $\tilde{c}_{m'}^*$, and $-\tilde{c}_{m'}^*$ [which represent $2(p-1)$ bits each] have the same $2(p-1)-2=2p-4$ MSBs. These common MSBs form exactly the bit sequence encapsulated by $\bar{b}_p^{(m)}$ (that corresponds to c_m) and which is represented by the blue-colored $\bar{b}_p^{(i,n)}$ in Fig. 2. By definition, they are also the only bits involved in the expression of $\mu_{k,p-1}(\tilde{c}_{m'})$:

$$\mu_{k,p-1}(\tilde{c}_{m'}) = \prod_{l=1}^{2(p-1)-2} e^{(2\bar{b}_l^{(m)}-1)\frac{L_l(k)}{2}}, \quad \forall \tilde{c}_{m'} \in \tilde{C}_{p-1}. \quad (31)$$

Now, injecting (31) in (11), we obtain the following recursive property:

$$\mu_{k,p}(\tilde{c}_m) = \mu_{k,p-1}(\tilde{c}_{m'}) \exp \left\{ (2\bar{b}_{2p-3}^{(i,n)} - 1)L_{2p-3}(k)/2 \right\} \\ \times \exp \left\{ (2\bar{b}_{2p-2}^{(i,n)} - 1)L_{2p-2}(k)/2 \right\}. \quad (32)$$

Clearly, one needs to further express the bits $\bar{b}_{2p-3}^{(i,n)}$ and $\bar{b}_{2p-2}^{(i,n)}$ (for each \tilde{c}_m in \tilde{C}_p) explicitly as function of i and n if $\mu_{k,p}(\tilde{c}_m)$ is to be split in terms of these two counters. If $\lfloor x \rfloor$ denotes the floor function that returns the largest integer smaller than or equal to x , the following lemma finds this useful decomposition.

Lemma 1: $\forall i, n = 1, 2, \dots, 2^{p-1}$, the two bits $\bar{b}_{2p-3}^{(i,n)}$ and $\bar{b}_{2p-2}^{(i,n)}$ are expressed as:

$$\bar{b}_{2p-2}^{(i,n)} = \left\lfloor \frac{i-1}{2^{p-2}} \right\rfloor \quad \text{and} \quad \bar{b}_{2p-3}^{(i,n)} = \left\lfloor \frac{n-1}{2^{p-2}} \right\rfloor. \quad (33)$$

Proof: See Appendix C.

Notice from (33) that $\bar{b}_{2p-2}^{(i,n)}$ and $\bar{b}_{2p-3}^{(i,n)}$ depend each on only one counter (either i or n). Therefore, we will from now on drop the vanishing counter in each of these two bits and they will be denoted simply by $\bar{b}_{2p-2}^{(i)}$ and $\bar{b}_{2p-3}^{(n)}$. Actually, a more general and much useful result can be stated here:

Assertion: All the odd-position bits, $\{\bar{b}_{2l-1}^{(i,n)}\}_{l=1}^p$, are function of n only and all the even-position bits, $\{\bar{b}_{2l}^{(i,n)}\}_{l=1}^p$, are function of i only. This is a direct consequence of the following *lemma*:

Lemma 2: The obtained 2^{2p} -QAM Gray-coded constellation has the following property:

- The odd-position bits, $\bar{b}_{2l-1}^{(i,n)}$, do not change by scanning each *horizontal* line of constellation points.
- The even-position bits, $\bar{b}_{2l}^{(i,n)}$, do not change by scanning each *vertical* line of constellation points.

Proof: This property is trivially verified for the *initial* QPSK depicted in Fig. 1(c). Now, assume that it is true at order $p-1$ (i.e., the previous $2^{2(p-1)}$ -QAM). Then, at order p , this property is automatically verified for the first $2p-2$ bits of all the obtained symbols. This is because the latter are obtained by placing the $2^{2(p-1)}$ -QAM as is in the top-right quadrant, \tilde{C}_p , and the other quadrants are obtained via the three symmetries of “step 2”. Moreover, since the basic QPSK from which the remaining two bits are copied verifies the underlying property, the latter becomes true for all the bits of the obtained constellation points.

In a nutshell, the fact that odd-position bits, $\bar{b}_{2l-1}^{(i,n)}$, do not change for each horizontal line means that they do not change by varying the symbols’ abscissa, $(2i-1)d_p$, or equivalently by changing the counter i . Therefore, $\{\bar{b}_{2l-1}^{(i,n)}\}_{l=1}^p$ are function of n only. The same reasons reveal that the even-position bits, $\{\bar{b}_{2l}^{(i,n)}\}_{l=1}^p$, are function of i only. This completes the proof of the assertion stated just before *Lemma 2*. As a consequence, we will from now on drop the vanishing counter from each group of bits and denote the latter, respectively, as $\bar{b}_{2l-1}^{(n)}$ and $\bar{b}_{2l}^{(i)}$ for $l = 1, 2, \dots, p$.

By revisiting (32) and considering the recursive construction of \tilde{C}_{p-1} (framed in blue color in Fig. 2) from the $2^{2(p-2)}$ -QAM constellation and following the same reasoning from (28) through (32), one can express $\mu_{k,p-1}(\tilde{c}_{m'})$ itself in the same recursive form of (32). We capitalize on this observation to show in Appendix D, by mathematical induction, the following theorem:

Theorem 1: For any $p \geq 2$, $\mu_{k,p}(\tilde{c}_m)$ can be factorized into two independent terms each of which depends solely on one of the two counters i and n as follows:

$$\mu_{k,p}(\tilde{c}_m) = \theta_{k,2p}(i)\theta_{k,2p-1}(n), \quad (34)$$

where $\theta_{k,2p}(i)$ and $\theta_{k,2p-1}(n)$ are expressed as:

$$\theta_{k,2p}(i) \triangleq \prod_{l=1}^{p-1} e^{(2\bar{b}_{2l}^{(i)}-1) \frac{L_{2l}(k)}{2}} \quad (35)$$

$$\theta_{k,2p-1}(n) \triangleq \prod_{l=1}^{p-1} e^{(2\bar{b}_{2l}^{(n)}-1) \frac{L_{2l-1}(k)}{2}}, \quad (36)$$

and they can be computed recursively, from lower-order constellations, for any $p \geq 2$ as follows:

$$\begin{aligned} \theta_{k,2p}(i) &= \theta_{k,2p-2} \left(\frac{|2i-1-2^{p-1}|+1}{2} \right) \\ &\times \exp \left\{ \left(2 \left\lfloor \frac{i-1}{2^{p-2}} \right\rfloor - 1 \right) \frac{L_{2p-2}(k)}{2} \right\}, \end{aligned} \quad (37)$$

$$\begin{aligned} \theta_{k,2p-1}(n) &= \theta_{k,2p-3} \left(\frac{|2n-1-2^{p-1}|+1}{2} \right) \\ &\times \exp \left\{ \left(2 \left\lfloor \frac{n-1}{2^{p-2}} \right\rfloor - 1 \right) \frac{L_{2p-3}(k)}{2} \right\}. \end{aligned} \quad (38)$$

Proof: See Appendix D.

Note that initialization in (37) and (38) is simply given by $\theta_{k,2}(1) = \theta_{k,1}(1) = 1$. This is because we extend the definition of $\mu_{k,p}(\cdot)$ for $p = 1$ (i.e., QPSK constellations) to be $\mu_{k,1}(c_m) = 1 \forall c_m \in C_1$ (cf. Section III). Hence, denoting the single symbol in \tilde{C}_1 as \tilde{c} , one can write $\mu_{k,1}(\tilde{c}) = \theta_{k,2}(1)\theta_{k,1}(1)$ as in (34) with $\theta_{k,2}(1) = \theta_{k,1}(1) = 1$.

Now, plugging (34) in (25) and using the fact that $\tilde{C}_p = \{(2i-1)d_p + j(2n-1)d_p\}_{i,n=1,2,\dots,2^{p-1}}$ and $|\tilde{c}_m|^2 = d_p^2([2i-1]^2 + [2n-1]^2)$, the term $D_\alpha(k)$ is rewritten as follows:

$$\begin{aligned} D_\alpha(k) &= 4\beta_k \sum_{i=1}^{2^{p-1}} \sum_{n=1}^{2^{p-1}} \left[\theta_{k,2p}(i) e^{-\rho d_p^2 (2i-1)^2} \right. \\ &\times \cosh \left(\frac{S(2i-1)d_p u(k)}{\sigma^2} + \frac{L_{2p}(k)}{2} \right) \\ &\times \theta_{k,2p-1}(n) e^{-\rho d_p^2 (2n-1)^2} \\ &\left. \times \cosh \left(\frac{S(2n-1)d_p v(k)}{\sigma^2} - \frac{L_{2p-1}(k)}{2} \right) \right]. \end{aligned} \quad (39)$$

Finally, after splitting the two sums in (39), $D_\alpha(k)$ is factorized as follows:

$$D_\alpha(k) = 4\beta_k F_{2p,\alpha}(u(k)) \times F_{2p-1,\alpha}(v(k)), \quad (40)$$

where the function $F_{q,\alpha}(\cdot)$ is given by:

$$\begin{aligned} F_{q,\alpha}(x) &= \sum_{i=1}^{2^{p-1}} \theta_{k,q}(i) e^{-\rho d_p^2 (2i-1)^2} \\ &\times \cosh \left(\frac{(2i-1)d_p Sx}{\sigma^2} + \frac{(-1)^q L_q(k)}{2} \right), \end{aligned} \quad (41)$$

in which q is a generic counter that is used, from now on, to refer to $2p$ or $2p-1$ depending on the context. This factorization is actually the cornerstone result behind enabling for the very first time the derivation of the analytical expressions for the considered stochastic CRLBs in the next section.

V. DERIVATION OF THE CLOSED-FORM EXPRESSIONS FOR THE CRLBS

Our starting point is the expression for the FIM elements defined in (4) and we are now ready to find the explicit expression for the global LLF of the system, $L(y; \alpha) \triangleq \ln(p[y; \alpha])$. In fact, by injecting (22) in (20), it follows that:

$$\begin{aligned} L(y; \alpha) &= -K \ln(2\pi\sigma^2) - \sum_{k=k_0}^{k_0+K-1} \frac{I(k)^2 + Q(k)^2}{2\sigma^2} \\ &\quad + \sum_{k=k_0}^{k_0+K-1} \ln(D_\alpha(k)). \end{aligned} \quad (42)$$

After using (40) in (42) and discarding the constant terms (that do not depend on ϕ and v), it follows that the *useful*¹⁰ LLF is decomposed as the sum of two analogous terms:

$$L(y; \alpha) = \sum_{k=k_0}^{k_0+K-1} [\ln(F_{2p,\alpha}(u(k))) + \ln(F_{2p-1,\alpha}(v(k)))]. \quad (43)$$

In the following, we will further show that the two random variables $u(k)$ and $v(k)$ are independent and *almost* identically distributed (i.e., their pdfs have the same structure, but they are parameterized differently). This is another interesting property that allows us to consider the term involving $u(k)$ only during all the derivation steps (partial derivatives and expectations). The results pertaining to the term involving $v(k)$ can then be deduced by easy identification (as will be seen later). In fact, injecting (40) in (22) and using the fact that $I(k)^2 + Q(k)^2 = u(k)^2 + v(k)^2$, it can be shown that $p[y(k); \alpha]$ itself is factorized as follows:

$$p[y(k); \alpha] = p[u(k); \alpha] p[v(k); \alpha], \quad (44)$$

¹⁰We will keep using the same notation, $L(y; \alpha)$, for both the *actual* and *useful* LLFs.

where the pdfs of $u(k)$ and $v(k)$ are given by:

$$p[u(k); \alpha] = \frac{2\beta_{k,2p}}{\sqrt{2\pi\sigma^2}} \exp\left\{-\frac{u(k)^2}{2\sigma^2}\right\} F_{2p,\alpha}(u(k)), \quad (45)$$

$$p[v(k); \alpha] = \frac{2\beta_{k,2p-1}}{\sqrt{2\pi\sigma^2}} \exp\left\{-\frac{v(k)^2}{2\sigma^2}\right\} F_{2p-1,\alpha}(v(k)), \quad (46)$$

with

$$\beta_{k,2p} = \frac{1}{2^p} \prod_{l=1}^p \frac{1}{\cosh(L_{2l}(k)/2)} \quad (47)$$

$$\beta_{k,2p-1} = \frac{1}{2^p} \prod_{l=1}^p \frac{1}{\cosh(L_{2l-1}(k)/2)}. \quad (48)$$

Moreover, we have $p[y(k) * e^{j(2\pi kv + \phi)}; \alpha] = p[u(k), v(k); \alpha]$ since $u(k)$ and $v(k)$ are indeed the real and imaginary parts of $y(k) * e^{j(2\pi kv + \phi)}$. Furthermore, since the synchronization parameters ϕ and \mathbf{v} are assumed to be deterministic, we readily have $p[y(k) * e^{j(2\pi kv + \phi)}; \alpha] = p[y(k)^*; \alpha] = p[y(k); \alpha]$. This leads to $p[u(k), v(k); \alpha] = p[y(k); \alpha]$ which is combined with (44) to yield:

$$p[u(k), v(k); \alpha] = p[u(k); \alpha] p[v(k); \alpha], \quad (49)$$

meaning that $u(k)$ and $v(k)$ are indeed two independent random variables (RVs) which are *almost* identically distributed according to (45) and (46). In the following, starting from (43), we will only detail the derivation of the first diagonal entry of the FIM for lack of space. The other entries can be found by following equivalent derivation steps. In fact, due to the *derivative* and *expectation* operators linearity, we readily have:

$$\begin{aligned} \mathbb{E}\left\{\frac{\partial^2 \ln(p[y; \alpha])}{\partial \phi^2}\right\} &= \sum_{k=k_0}^{k_0+K-1} \mathbb{E}\left\{\frac{\partial^2 \ln(F_{2p,\alpha}(u(k)))}{\partial \phi^2}\right\} \\ &+ \sum_{k=k_0}^{k_0+K-1} \mathbb{E}\left\{\frac{\partial^2 \ln(F_{2p-1,\alpha}(v(k)))}{\partial \phi^2}\right\}. \end{aligned} \quad (50)$$

Again, due to the apparent symmetries between the pdfs of $u(k)$ and $v(k)$ in (45) and (46), we will detail the derivation of the term involving $u(k)$ only, which is denoted hereafter as $\gamma_{k,2p} \triangleq \mathbb{E}\{\partial^2 \ln(F_{2p,\alpha}(u(k))) / \partial \phi^2\}$. Then, its equivalent term $\gamma_{k,2p-1} \triangleq \mathbb{E}\{\partial^2 \ln(F_{2p-1,\alpha}(v(k))) / \partial \phi^2\}$ can be easily deduced, at the very end, by simple identification.

To do so, we denote the first and second derivatives of $F_{2p,\alpha}(x)$ with respect to the working variable x by $F'_{2p,\alpha}(x)$ and $F''_{2p,\alpha}(x)$, respectively (their expressions are provided in Appendix F). Moreover, from (26) and (27), we readily have:

$$u'(k) \triangleq \partial u(k) / \partial \phi = -v(k) \text{ and } v'(k) \triangleq \partial v(k) / \partial \phi = u(k), \quad (51)$$

from which we obtain $u''(k) = -u(k)$. Using this result, we show after some algebraic manipulations that:

$$\begin{aligned} \frac{\partial^2 \ln(F_{2p,\alpha}(u(k)))}{\partial \phi^2} &= -u(k) \frac{F'_{2p,\alpha}(u(k))}{F_{2p,\alpha}(u(k))} \\ &+ v(k)^2 \left[\frac{F''_{2p,\alpha}(u(k))}{F_{2p,\alpha}(u(k))} - \left(\frac{F'_{2p,\alpha}(u(k))}{F_{2p,\alpha}(u(k))} \right)^2 \right]. \end{aligned} \quad (52)$$

Then, since $u(k)$ and $v(k)$ are independent RVs, it follows that:

$$\begin{aligned} \gamma_{k,2p} &= -\mathbb{E}\left\{u(k) \frac{F'_{2p,\alpha}(u(k))}{F_{2p,\alpha}(u(k))}\right\} \\ &+ \mathbb{E}\{v(k)^2\} \left[\mathbb{E}\left\{\frac{F''_{2p,\alpha}(u(k))}{F_{2p,\alpha}(u(k))}\right\} - \mathbb{E}\left\{\left(\frac{F'_{2p,\alpha}(u(k))}{F_{2p,\alpha}(u(k))}\right)^2\right\} \right]. \end{aligned} \quad (53)$$

These are expectations of random variable transformations involving either $u(k)$ or $v(k)$ separately. Since the pdfs of these two RVs were already established in (45) and (46), these expectations can be expressed in closed form. For instance, by integrating over the pdf of $v(k)$, it follows that:

$$\begin{aligned} \mathbb{E}\{v(k)^2\} &= \int_{-\infty}^{\infty} v(k)^2 p[v(k); \alpha] dv(k) \\ &= \frac{2\beta_{k,2p-1}}{\sqrt{2\pi\sigma^2}} \int_{-\infty}^{\infty} v(k)^2 F_{2p-1,\alpha}(v(k)) e^{-\frac{v(k)^2}{2\sigma^2}} dv(k). \end{aligned} \quad (54)$$

After expanding the expression of $F_{2p-1}(x)$ in (41) using the identity $\cosh(x+y) = \sinh(x)\sinh(y) + \cosh(x)\cosh(y)$, inverting the sum and integral signs, and then resorting to some algebraic manipulations, it can be shown that:

$$\begin{aligned} \mathbb{E}\{v(k)^2\} &= 2\beta_{k,2p-1} \cosh\left(\frac{L_{2p-1}(k)}{2}\right) \\ &\times \sum_{n=1}^{2^{p-1}} \theta_{k,2p-1}(n) [\sigma^2 + S^2 d_p^2 (2n-1)^2] \\ &= \sigma^2 \left[\rho \omega_{k,2p-1} + 2\beta_{k,2p-1} \cosh\left(\frac{L_{2p-1}(k)}{2}\right) \right. \\ &\quad \left. \times \sum_{n=1}^{2^{p-1}} \theta_{k,2p-1}(n) \right], \end{aligned} \quad (55)$$

in which $\omega_{k,2p-1}$ and $\omega_{k,2p}$ that will appear shortly are common coefficients to all FIM elements given by:

$$\omega_{k,r} \triangleq 4a_p^2 \beta_{k,r} \cosh(L_r(k)/2) \sum_{i=1}^{2^{p-1}} (2i-1)^2 \theta_{k,r}(i), \quad (56)$$

where r is either $2p$ or $2p-1$. We further simplify (55) by using the following lemma:

Lemma 3: Recalling the expression of $\beta_{k,2p-1}$ in (47), we have:

$$2\beta_{k,2p-1} \cosh(L_{2p-1}(k)/2) \sum_{n=1}^{2^{p-1}} \theta_{k,2p-1}(n) = 1. \quad (57)$$

Proof: See Appendix E.

In fact, by plugging (57) in (55), it follows that:

$$\mathbb{E}\{v(k)^2\} = \sigma^2 [1 + \rho \omega_{k,2p-1}]. \quad (58)$$

The closed-form expressions for the other expectations involved in (53) are derived in Appendix F, by integrating over the pdf of $u(k)$. The final results are as follows:

$$\mathbb{E} \left\{ u(k) \frac{F_{2p,\alpha}(u(k))}{F_{2p,\alpha}(u(k))} \right\} = \rho \omega_{k,2p}, \quad (59)$$

$$\mathbb{E} \left\{ \frac{F''_{2p,\alpha}(u(k))}{F_{2p,\alpha}(u(k))} \right\} = \frac{\omega_{k,2p}}{\sigma^2} \rho, \quad (60)$$

$$\mathbb{E} \left\{ \left(\frac{F'_{2p,\alpha}(u(k))}{F_{2p,\alpha}(u(k))} \right)^2 \right\} = \frac{4d_p^2 \beta_{k,2p}}{\sigma^2} \rho \Psi_{k,2p}(\rho), \quad (61)$$

where in the last equality $\Psi_{k,2p}(\cdot)$ is given by:

$$\Psi_{k,2p}(\rho) = \frac{1}{\sqrt{2\pi}} \int_{-\infty}^{+\infty} \frac{\lambda_{k,2p}^2(t, \rho)}{\delta_{k,2p}(t, \rho)} e^{-\frac{t^2}{2}} dt \quad (62)$$

with

$$\begin{aligned} \lambda_{k,2p}(t, \rho) &= \sum_{i=1}^{2p-1} (2i-1) \theta_{k,2p}(i) e^{-(2i-1)^2 d_p^2 \rho} \\ &\quad \times \sinh \left(\sqrt{2\rho} (2i-1) d_p t + L_{2p}(k)/2 \right), \\ \delta_{k,2p}(t, \rho) &= \sum_{i=1}^{2p-1} \theta_{k,2p}(i) e^{-(2i-1)^2 d_p^2 \rho} \\ &\quad \times \cosh \left(\sqrt{2\rho} (2i-1) d_p t + L_{2p}(k)/2 \right). \end{aligned} \quad (63)$$

Therefore, by injecting the four expectations evaluated in (58) to (61) back into (53), the first term in (50) earlier denoted as $\gamma_{k,2p} \triangleq \mathbb{E} \left\{ \partial^2 \ln(F_{2p,\alpha}(u(k))) / \partial \phi^2 \right\}$ is obtained as follows:

$$\gamma_{k,2p}(\rho) = \omega_{k,2p-1} \rho \left[\omega_{k,2p} \rho - 4d_p^2 \beta_{k,2p} \Psi_{2p}(\rho) \left(\frac{1}{\omega_{k,2p-1}} + \rho \right) \right]. \quad (64)$$

As mentioned previously, the expression of the second term, $\gamma_{k,2p-1} \triangleq \mathbb{E} \left\{ \partial^2 \ln(F_{2p-1,\alpha}(v(k))) / \partial \phi^2 \right\}$, involved in (50) can be easily deduced from the expression of $\gamma_{k,2p}(\rho)$ in (64). This is due to the apparent symmetries in the pdfs of the two RVs $u(k)$ and $v(k)$, as seen from (45) and (46), leading to:

$$\begin{aligned} \gamma_{k,2p-1}(\rho) &= \omega_{k,2p} \rho \left[\omega_{k,2p-1} \rho - 4d_p^2 \beta_{k,2p-1} \Psi_{2p-1}(\rho) \left(\frac{1}{\omega_{k,2p}} + \rho \right) \right]. \end{aligned} \quad (65)$$

Lastly, the first diagonal element of the FIM follows immediately from (50) as follows:

$$-\mathbb{E} \left\{ \frac{\partial^2 \ln(p[y; \alpha])}{\partial \phi^2} \right\} = - \sum_{k=k_0}^{k_0+K-1} [\gamma_{2p,k}(\rho) + \gamma_{2p-1,k}(\rho)]. \quad (66)$$

Deriving the other elements using equivalent manipulations¹¹ and defining $\Omega_{p,k}(\rho) \triangleq -\gamma_{2p,k}(\rho) - \gamma_{2p-1,k}(\rho)$, we obtain an analytical expression for the FIM in CA estimation as follows:

$$I(\alpha) = \sum_{k=k_0}^{k_0+K-1} \Omega_{p,k}(\rho) \begin{pmatrix} 1 & 2\pi k \\ 2\pi k & (2\pi)^2 k^2 \end{pmatrix} = \sum_{k=k_0}^{k_0+K-1} I_k(\alpha), \quad (67)$$

where $I_k(\alpha)$ is the FIM pertaining to the k^{th} received sample. Note that the term $2\pi k$ in the off-diagonal elements of $I(\alpha)$ stems from the partial derivative of $u(k)$ and $v(k)$ with respect to ν which are obtained, respectively, from (26) and (27) as $\partial u(k)/\partial \nu = -2\pi k v(k)$ and $\partial v(k)/\partial \nu = 2\pi k u(k)$. Obviously, the term $(2\pi k)^2$ in the first diagonal element of the FIM stems from the second partial derivatives of these two quantities with respect to ν . Note also that the per-sample FIM, $I_k(\alpha)$, is not invertible due to the linear dependence of its two columns within a factor $2\pi k$. This means that the carrier phase and the CFO cannot be *jointly* estimated using a single received sample. This is hardly surprising, since $y(k)$ depends on ν and ϕ through the transformation $[0 \ 2\pi \times \mathbb{R}_+ \rightarrow \mathbb{C} : (\phi, \nu) \rightarrow e^{j(2\pi \nu k + \phi)}$ which does not entail a one-to-one (or injective) mapping. In plain English, two different couples (ϕ_1, ν_1) and (ϕ_2, ν_2) can yield the same received sample, $y(k)$, and no estimator is ever able to separate them based solely on $y(k)$. Take, however, any two different samples [say $y(k_1)$ and $y(k_2)$ with $k_1 \neq k_2$] and it can be verified that $I_{k_1}(\alpha) + I_{k_2}(\alpha)$ is always invertible.

Now, the obtained general FIM expression (67), in CA estimation, encloses the two traditional (extreme) scenarios of *completely NDA* and *completely DA* estimations as special cases. Indeed, in the former case, no *a priori* information about the bits is available at the receiver end and, therefore, $Pr[b_l^k = 1] = Pr[b_l^k = 0] = 1/2$ thereby yielding $L_l^{\text{NDA}}(k) = 0$ for all l and k . In the latter case, however, the bits are *a priori* perfectly known and, therefore, at the receiver side we have either $\{Pr[b_l^k = 1] = 1 \text{ hence } Pr[b_l^k = 0] = 0\}$ or $\{Pr[b_l^k = 0] = 1 \text{ hence } Pr[b_l^k = 1] = 0\}$ and consequently the LLRs verify $L_l^{\text{DA}}(k) = \pm\infty$. By injecting these two typical values, $L_l^{\text{NDA}}(k)$ and $L_l^{\text{DA}}(k)$, in all the quantities that are involved in the entries of $I_k(\alpha)$ and by recurring to some easy simplifications, one obtains exactly the same expressions for the FIMs developed earlier in [26] and [43] in the traditional NDA and DA cases, respectively.

The CRLBs for the phase shift and the CFO are, respectively, the first and second diagonal elements of the FIM inverse $I^{-1}(\alpha)$. As such, their closed-form expressions in CA estimation are established as follows: We stress here the fact that the FIM associated with the synchronization parameters depends on the first time index k_0 as seen from (67). Such dependencies on the observation window have previously been reported in the literature even in the NDA case [24]–[26]. In CA estimation as well, we obtain different loose (or excessively optimistic) bounds as k_0 varies. Our interest is focused on the tightest bound which is obtained when the square of the off-diagonal elements is negligible compared to the product of the diagonal ones:

$$0 \leq [I(\alpha)]_{1,2}^2 \ll [I(\alpha)]_{1,1} [I(\alpha)]_{2,2}. \quad (70)$$

¹¹Details were omitted due to lack of space.

We verify by simulations that the off-diagonal entries are close to zero when the set of sampling indices is centred around zero, i.e., $k_0 = -\frac{K-1}{2}$. In this case, the CRLBs' expressions in (68) and (69), shown at the bottom of the page, reduce to:

$$\text{CRLB}_{\text{CA}}(\mathbf{v}) = \frac{1}{(2\pi)^2} \left(\sum_{k=-\frac{K-1}{2}}^{\frac{K-1}{2}} \Omega_{p,k}(\rho) k^2 \right)^{-1} \quad (71)$$

$$\text{CRLB}_{\text{CA}}(\phi) = \left(\sum_{k=-\frac{K-1}{2}}^{\frac{K-1}{2}} \Omega_{p,k}(\rho) \right)^{-1}. \quad (72)$$

Finally, it is worth mentioning that the CRLB expressions established in (68), (69) and (71) apply for LDPC codes in conjunction with Turbo processing as well. In fact, all the algebraic manipulations we used to establish such expressions involve the actual APPs of the coded bits (which are expressed in terms of their LLRs). Only during the evaluation of the CRLBs do we need the estimates for such LLRs. In Turbo codes, the LLRs are accurately approximated by the *extrinsic* information delivered by the decoder. When used in conjunction with turbo processing, LDPC-coded systems as well provide the *extrinsic* information at the output of the MAP SISO decoder. Such *extrinsic* information is again a good approximation for the bit LLRs and can, therefore, be used to evaluate the underlying CA CRLBs for LDPC systems [38], [39].

VI. EXTENSION TO MULTICARRIER SYSTEMS

All the above derivations are valid for a single-carrier *flat-fading* channel, i.e., in the absence of multipath fading. Yet in the presence of multipath fading, it is well known that OFDM—a key feature of current- and next-generation systems—transforms the *frequency-selective* channel in the time domain into a set of parallel *flat-fading* channels over each subcarrier in the frequency domain [34], [35]. In fact, consider a multicarrier system consisting of Q tones. At the receiver side, after removing the cyclic prefix and performing the FFT, the K received samples over each $\{q^{\text{th}}\}_{q=1}^Q$ subcarrier are given by:

$$y_q(k) = S_q x(k) e^{j(2\pi k v + \phi_q)} + w_q(k), \quad k = k_0, k_0 + 1, \dots, k_0 + K - 1, \quad (73)$$

where S_q and ϕ_q are, respectively, the *real* channel coefficient and the phase shift corresponding to the q^{th} subcarrier (i.e., $S_q e^{j\phi_q}$ is the flat-fading complex channel frequency response over that subcarrier). In (73), the components $\{w_q(k)\}$ model the combined effects of the background thermal noise and the

inter-carrier interference (ICI) that arises from the presence of the CFO. Now, we have $Q + 1$ unknown synchronization parameters to be estimated which are the Q phase distortions, $\{\phi_q\}_{q=1}^Q$, and the CFO, \mathbf{v} , which is the same for all the subcarriers. These parameters are gathered in a single vector $\alpha = [\phi_1, \phi_2, \dots, \phi_Q, \mathbf{v}]$. Moreover, the *frequency-domain* received samples over each subcarrier in (73) are gathered in a single vector $y_q = [y_q(k_0), y_q(k_0 + 1), \dots, y_q(k_0 + K - 1)]^T$ and the received samples over all the subcarriers are stacked in a single observation matrix, Y , whose q^{th} row is given by y_q^T . Due to the independence of the noise components and the transmitted symbols across subcarriers, the pdf of Y parameterized by α is simply given by:

$$p[Y; \alpha] = \prod_{q=1}^Q p[y_q; \alpha_q], \quad (74)$$

where $\alpha_q = [\phi_q, \mathbf{v}]$. Consequently, the *global* LLF of the system is obtained as:

$$\mathcal{L}(Y; \alpha) = \sum_{q=1}^Q \mathcal{L}(y_q; \alpha_q). \quad (75)$$

This means that the *global* LLF is simply the sum of the *elementary* LLFs, $\{\mathcal{L}(y_q; \alpha_q)\}_{q=1}^Q$, that we already established in (43) and that are obtained by considering the samples received over each subcarrier alone (i.e., in a traditional *single-carrier* system, *hypothetically*). Therefore, owing to the linearity of the second partial derivative and statistical expectation operators, it can be easily seen from (75) that the entries of the $(Q + 1) \times (Q + 1)$ *global* FIM can be directly deduced from the entries of the *elementary* (i.e., single-carrier) FIM already derived in Section V. In fact, by defining $\rho_q = S_q^2 / 2\sigma^2$ to be the signal-to-noise-plus-interference ratio (SINR) on the q^{th} subcarrier, we obtain for for $q, q' = 1, 2, \dots, Q$:

$$[I(\alpha)]_{\phi_q, \phi_q} = -E \left\{ \frac{\partial^2 \ln(p[Y; \alpha])}{\partial \phi_q^2} \right\} = \sum_{k=k_0}^{k_0+K-1} \Omega_{p,k}(\rho_q), \quad (76)$$

$$\begin{aligned} [I(\alpha)]_{\mathbf{v}, \mathbf{v}} &= -E \left\{ \frac{\partial^2 \ln(p[Y; \alpha])}{\partial \mathbf{v} \partial \mathbf{v}} \right\} \\ &= (2\pi)^2 \sum_{q=1}^Q \sum_{k=k_0}^{k_0+K-1} \Omega_{p,k}(\rho_q) k^2, \end{aligned} \quad (77)$$

$$\text{CRLB}_{\text{CA}}(\mathbf{v}) = \frac{1}{(2\pi)^2} \frac{\sum_{k=k_0}^{k_0+K-1} \Omega_{p,k}(\rho)}{\left(\sum_{k=k_0}^{k_0+K-1} \Omega_{p,k}(\rho) \right) \left(\sum_{k=k_0}^{k_0+K-1} \Omega_{p,k}(\rho) k^2 \right) - \left(\sum_{k=k_0}^{k_0+K-1} \Omega_{p,k}(\rho) k \right)^2}, \quad (68)$$

$$\text{CRLB}_{\text{CA}}(\phi) = \frac{\sum_{k=k_0}^{k_0+K-1} \Omega_{p,k}(\rho) k^2}{\left(\sum_{k=k_0}^{k_0+K-1} \Omega_{p,k}(\rho) \right) \left(\sum_{k=k_0}^{k_0+K-1} \Omega_{p,k}(\rho) k^2 \right) - \left(\sum_{k=k_0}^{k_0+K-1} \Omega_{p,k}(\rho) k \right)^2} \quad (69)$$

$$\begin{aligned}
[I(\alpha)]_{\nu, \phi_q} &= -E \left\{ \frac{\partial^2 \ln(p[Y; \alpha])}{\partial \nu \partial \phi_q} \right\} \\
&= 2\pi \sum_{q=1}^Q \sum_{k=k_0}^{k_0+K-1} \Omega_{p,k}(\rho_q) k, \quad (78)
\end{aligned}$$

$$[I(\alpha)]_{\phi_q, \phi_{q'}} = -E \left\{ \frac{\partial^2 \ln(p[Y; \alpha])}{\partial \phi_q \partial \phi_{q'}} \right\} = 0. \text{ (for } q \neq q') \quad (79)$$

As different loose bounds are obtained for different values of k_0 , we seek the tightest bound obtained when $k_0 = -\frac{K-1}{2}$ (for the same reasons already explained in Section V). Indeed, for this typical value, the *off-diagonal* elements in (78) are almost equal to zero. And since the remaining off-diagonal elements in (79) are already identically zero, the *global* FIM becomes diagonal. Therefore, the CRLB associated to each of the $Q+1$ synchronization parameters is simply obtained by inverting the corresponding diagonal entry, i.e.,¹²

$$\text{CRLB}_{\text{CA}}^{\text{MC}}(\nu) = \frac{1}{(2\pi)^2} \left(\sum_{q=1}^Q \sum_{k=-\frac{K-1}{2}}^{\frac{K-1}{2}} \Omega_{p,k}(\rho_q) k^2 \right)^{-1}, \quad (80)$$

$$\text{CRLB}_{\text{CA}}^{\text{MC}}(\phi_q) = \left(\sum_{k=-\frac{K-1}{2}}^{\frac{K-1}{2}} \Omega_{p,k}(\rho_q) \right)^{-1} \text{ for } q = 1, 2, \dots, Q.$$

(81)

Note from (81) that the CRLB of the phase shift on each q^{th} subcarrier, in a *multi-carrier* system, is equivalent to its counterpart in a *single-carrier* system that was already established in the right-hand side of (71). This is hardly surprising since the phase shift associated to each subcarrier is involved in the samples received over that subcarrier only as seen from (73). Being common to all subcarriers, the CFO is, however, involved in the received samples over all the subcarriers and thus its CRLB in a multi-carrier system (80) is not equivalent to but actually lower than its counterpart in a single-carrier system (71). To see this, assume that all the subcarriers have the same modulation order (p), coding rate (R), and exhibit almost the same SNR level (ρ), i.e., $(p_q, R_q, \rho_q) = (p, R, \rho)$ for all $q = 1, 2, \dots, Q$. Then, all the CFO CRLBs, $\{\text{CRLB}_{\text{CA}}^{(q)}(\nu)\}_{q=1}^Q$, that would be obtained by considering the K received samples over each subcarrier alone [established in the left-hand side of (71)] are the same and are given for $q = 1, 2, \dots, Q$ by:

$$\begin{aligned}
[\text{CRLB}_{\text{CA}}^{(q)}(\nu)]^{-1} &= (2\pi)^2 \sum_{k=-\frac{K-1}{2}}^{\frac{K-1}{2}} \Omega_{p,k}(\rho_q) k^2 \\
&= (2\pi)^2 \sum_{k=-\frac{K-1}{2}}^{\frac{K-1}{2}} \Omega_{p,k}(\rho) k^2 \\
&\triangleq [\text{CRLB}_{\text{CA}}(\nu)]^{-1}. \quad (82)
\end{aligned}$$

¹²Note here that the established CA CRLBs remain valid in multiple-input multiple-output (MIMO) communications under frequency-flat channels or MIMO-ODM communications under frequency-selective channels both with orthogonal spatial precoding. As a matter of fact, OFDM itself can be regarded here as an orthogonal precoding scheme.

Consequently, injecting (82) in (80), it follows that the CFO CRLB in a multi-carrier system is obtained as:

$$\text{CRLB}_{\text{CA}}^{\text{MC}}(\nu) = \left(\sum_{q=1}^Q \frac{1}{\text{CRLB}_{\text{CA}}^{(q)}(\nu)} \right)^{-1} = \frac{\text{CRLB}_{\text{CA}}(\nu)}{Q}. \quad (83)$$

Besides, it is also worth mentioning that the two CRLB expressions in multi-carrier systems obtained in (80) and (81) remain valid in the more general AMC case when the modulation order, p , and coding rate, R , may vary from one subcarrier to another depending on the corresponding CQI. In this case, as well, we have:

$$\sum_{q=1}^Q \sum_{k=-\frac{K-1}{2}}^{\frac{K-1}{2}} \Omega_{p,k}(\rho_q) k^2 \geq \min_{q=1,2,\dots,Q} \left\{ \sum_{k=-\frac{K-1}{2}}^{\frac{K-1}{2}} \Omega_{p,k}(\rho_q) k^2 \right\}. \quad (84)$$

Thus, it follows from (80) that:

$$\begin{aligned}
\text{CRLB}_{\text{CA}}^{\text{MC}}(\nu) &\leq \min_{q=1,2,\dots,Q} \left\{ \left((2\pi)^2 \sum_{k=-\frac{K-1}{2}}^{\frac{K-1}{2}} \Omega_{p,k}(\rho_q) k^2 \right)^{-1} \right\} \\
&= \min_{q=1,2,\dots,Q} \left\{ \text{CRLB}_{\text{CA}}^{(q)}(\nu) \right\} \leq \text{CRLB}_{\text{CA}}^{(q)}(\nu) \forall q,
\end{aligned}$$

meaning that, in the AMC scheme as well, the CFO CRLB in a multi-carrier system is lower than its counterpart in a single-carrier system.

VII. SIMULATION RESULTS

In this section, we provide graphical representations for the analytical CRLBs in (71) for the joint estimation of the synchronization parameters, with different modulation orders and different coding rates. The encoder is composed of two identical RSCs concatenated in parallel, of generator polynomials (1, 0, 1, 1) and (1, 1, 0, 1), with systematic rate $R_0 = \frac{1}{2}$ each. The output of the turbo encoder is punctured to achieve the desired code rate R . For the tailing bits, the size of the RSC encoders memory is fixed to 4. To evaluate the obtained CA estimation CRLBs, the extrinsic information delivered by the SISO decoder is used to evaluate the *a priori* bit LLRs, $L_l(k)$. Note that having the *a priori* LLRs at hand, it is possible to evaluate all the quantities involved in the expressions of the considered bounds. Indeed, as pointed out in [11], [40], [41] (and references therein) and owing to the turbo principle, the extrinsic information obtained at steady state accurately approximates the bit's *a priori* LLRs, $L_l(k)$ for all l and k , that are involved in the new CA CRLBs expressions.

For every bit, b_l^k , the corresponding $L_l(k)$ that is used in our simulations are obtained as the difference, i.e., $L_l(k) = Y_l(k) - \Lambda_l(k)$ where $Y_l(k)$ is the *a posteriori* LLR of b_l^k that is delivered by the decoder at steady state and whose sign is usually used for detecting that same bit. $\Lambda_l(k)$, however, is the soft likelihood value that is fed as input to the decoder before starting the iterative turbo exchange process. Note that in higher order QAMs, these $\Lambda_l(k)$ are delivered by the *soft* demapper

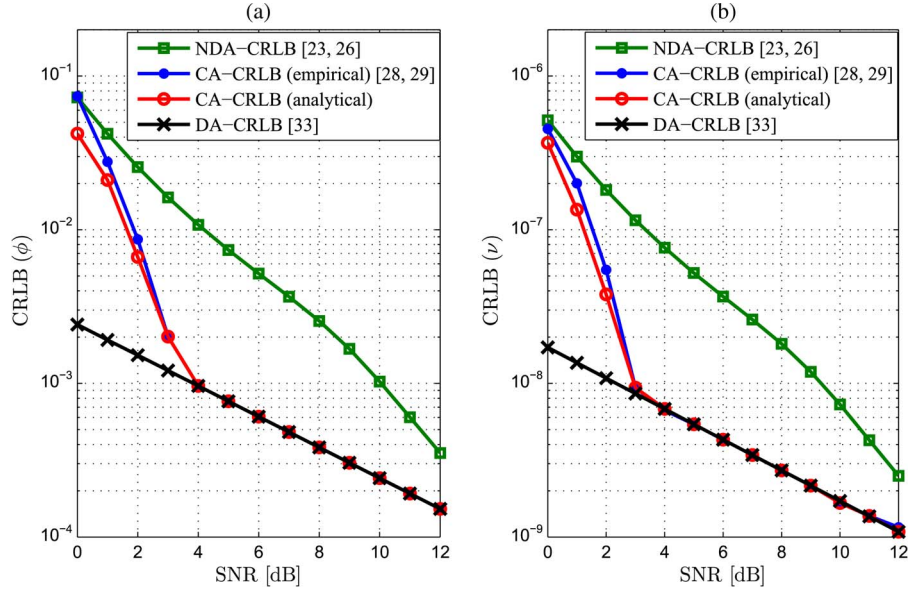


Fig. 3. NDA, DA, and CA (analytical and empirical) estimation CRLBs for: (a) the phase shift, and (b) the CFO (16-QAM; $K = 207$).

that is placed just before the turbo decoder. In all simulations, we used the $L_l(k)$ obtained at the 10th turbo iteration. Moreover, since the values of all the obtained $L_l(k)$ depend on the underlying noise realization, the new analytical CA CRLBs are also averaged over a small number of noise realization, at every SNR point, to smoothen the curve. Typically, in our paper, they were smoothed over 20 realizations.

Moreover, notice that the obtained CA CRLB expressions do not depend on the true values of the unknown phase shift and CFO. Hence, they do hold the same for all the possible values of these synchronization parameters. Thus, in our simulations, we evaluate the CA CRLBs for $\phi = 0$ and $\nu = 0$ which provide the most reliable values for the LLRs. Yet, even in presence of non-zero values for ϕ and ν , it is the derotated samples, $y(k)e^{-j(\phi+2\pi k\nu)}$, that should be fed to the decoder and not $y(k)$. This is because, unlike practical estimators where these parameters are actually unknown, the CRLB is a fundamental bound that is evaluated at the true values of the unknown parameters, i.e., as if we know ϕ and ν which can then be used for data derotation. This brings the whole situation back to the case where $\phi = 0$ and $\nu = 0$ and thus to the most reliable LLRs (that we used in our simulations).

In Fig. 3, we verify that the new closed-form CRLBs coincide with their *empirical* counterparts obtained in [33], [36] but from exhaustive Monte-Carlo simulations (20 000 runs in our results). Hence, the new analytical expressions corroborate these previous attempts to evaluate the considered bounds *empirically* and allow their immediate evaluation for any square-QAM turbo-coded signal.

As expected, we also see from the same figure that the CA CRLBs are smaller than the NDA CRLBs which were earlier introduced in [23], [26]. This highlights the performance improvements that can be achieved by a coded system over an uncoded one. For example, at SNR = 4 dB, the CA CRLBs are about up to 10 times smaller than the NDA CRLBs. This figure underlines the huge potential performance gain that

could be achieved at such low SNR level. Additionally and most prominently, the CA CRLBs decrease rapidly and reach the DA CRLBs which are the ideal bounds that would be obtained if all the transmitted symbols were perfectly known to the receiver, and which are simply given by [43]:

$$\text{CRLB}_{\text{DA}}(\nu) = \frac{6}{(2\pi)^2 K(K^2 - 1)\rho}, \quad (85)$$

$$\text{CRLB}_{\text{DA}}(\phi) = \frac{1}{2K\rho}. \quad (86)$$

In Fig. 4, we plot the CA CRLBs for different modulation orders. It is clear that the CRLBs increase with the modulation order at a given SNR value. This is a typical behavior that was observed for NDA CRLBs, as well, and actually for any parameter estimation problem involving linearly-modulated signals. Indeed, when the modulation order increases, the intersymbol distance decreases for normalized-energy constellations. As such, at the same SNR level, noise components have a relatively worse impact on symbol detection and parameter estimation in general. Furthermore, even in probability theory, when the ambient sample space of the *nuisance* parameters (here the constellation alphabet) gets larger, more uncertainty is introduced about each transmitted symbol thereby rendering estimation more difficult. Another interesting observation which can be drawn from Fig. 4 is that the CRLB for the frequency is much smaller than that for the phase. This is simply because the received signal depends much more on ν than on ϕ through the time index k in the argument of $e^{j(2\pi\nu k + \phi)}$. In other words, the received samples carry more information on the frequency than on the phase.

In Fig. 5, we show the effect of the coding rate on the synchronization performance. In fact, we plot the CA CRLBs for the carrier phase estimation using two different coding rates $R_1 = 0.3285 \approx \frac{1}{3}$ and $R_2 = 0.4892 \approx \frac{1}{2}$. Even though both CA CRLBs coincide at moderate SNRs, they exhibit a significant

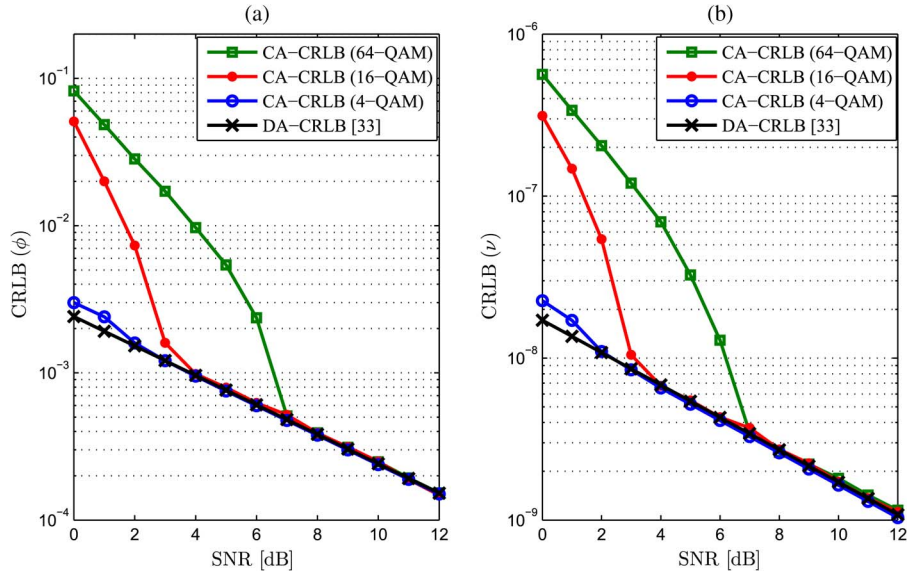


Fig. 4. CA estimation CRLBs (analytical) for: (a) the phase shift, and (b) the CFO (4-, 16-, and 64-QAM; $K = 207$).

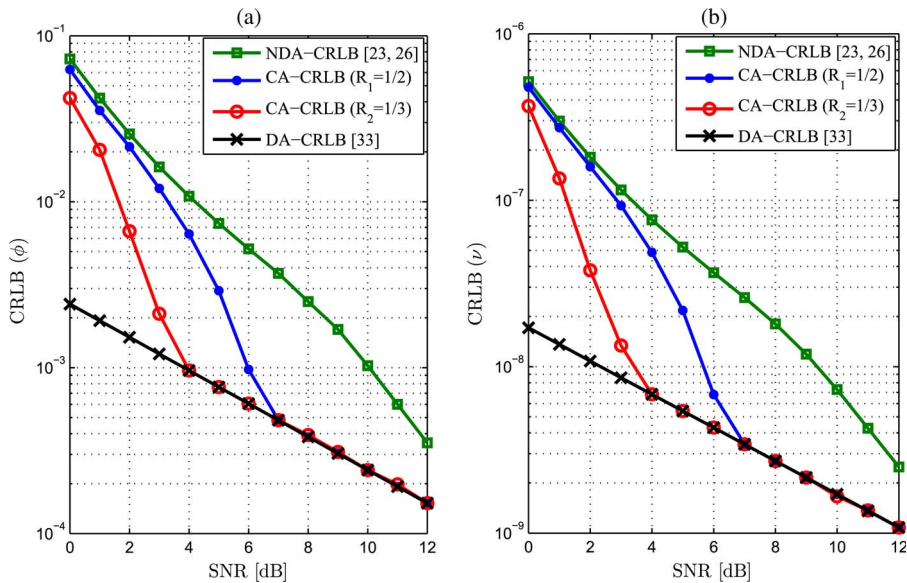


Fig. 5. CA estimation CRLBs (analytical) for: (a) the phase shift, and (b) the CFO ($R_1 = 1/2$, $R_2 = 1/3$; 16-QAM; $K = 207$).

gap at lower SNR levels. In fact, with smaller coding rates, more redundancy is provided by the turbo encoder. Consequently, the decoder is more likely able to correctly detect the transmitted bits enhancing thereby the estimation performance.

VIII. CONCLUSION

In this paper, we derived for the first time analytical expressions for the CRLBs of joint CFO and carrier phase estimation from turbo-coded square-QAM-modulated single- or multi-carrier transmissions. In the latter case, the newly derived bounds remain valid in the more general AMC case where the coding rate and modulation order vary from one subcarrier to another depending on the corresponding CQI. Our new analytical bounds coincide with their empirical counter-

parts earlier computed in [33], [36] in the single-carrier case only. They are also remarkably smaller than the NDA CRLBs thereby suggesting enhanced synchronization capabilities if the *soft* information provided by the turbo decoder is exploited during the estimation process. Moreover, the CA CRLBs decay rapidly with the SNR and reach the DA CRLB at relatively low thresholds where all the transmitted symbols are assumed to be perfectly known. The effect of the coding rate is also more apparent in the low SNR regime where more redundancy implies more accurate decoding and therefore better synchronization. It was also shown that contrarily to the CRLB of the phase shift, the CRLB of the CFO improves in a multi-carrier system as compared to its counterpart in a single-carrier system. Finally, the new CA CRLBs are also valid for LDPC-coded systems when the latter are used in conjunction with turbo processing.

APPENDIX A

It is easy to show that the new recursive process yields Gray-coded constellations. In fact, pick up any two closest points, c_{m_1} and c_{m_2} , from the obtained 2^{2p} -QAM constellation (i.e., verifying $|c_{m_1} - c_{m_2}| = 2d_p$ with $2d_p$ being the intersymbol distance). If c_{m_1} and c_{m_2} belong to the same quadrant, then in light of "step 3" they share the same two least significant bits (LSBs), i.e., $\bar{b}_{2p}^{m_1} = \bar{b}_{2p}^{m_2}$ and $\bar{b}_{2p-1}^{m_1} = \bar{b}_{2p-1}^{m_2}$. Moreover, the truncated sequences built from the remaining bits (denoted as $\bar{b}_p^{m_1} \triangleq \bar{b}_1^{m_1} \bar{b}_2^{m_1} \dots \bar{b}_{2p-2}^{m_1}$ and $\bar{b}_p^{m_2} \triangleq \bar{b}_1^{m_2} \bar{b}_2^{m_2} \dots \bar{b}_{2p-2}^{m_2}$) correspond to two closest points in the previous Gray-coded $2^{2(p-1)}$ -QAM constellation (see "step 1", "step 2" and footnote 5). Thus, $\bar{b}_p^{m_1}$ and $\bar{b}_p^{m_2}$ differ by one bit only and thus this property holds true for the whole bit sequences $\bar{b}_p^{m_1} \bar{b}_{2p-2}^{m_1} \bar{b}_{2p-1}^{m_1}$ and $\bar{b}_p^{m_2} \bar{b}_{2p-2}^{m_2} \bar{b}_{2p-1}^{m_2}$ (corresponding to c_{m_1} and c_{m_2}). Now, if c_{m_1} and c_{m_2} do not belong to the same quadrant, then the fact that $|c_{m_1} - c_{m_2}| = 2d_p$ (closest points) implies that they are symmetrical with respect to either the x -axis or the y -axis (belonging to two adjacent quadrants). Thus, according to "step 2", they share the same first $2p - 2$ bits, i.e., $\bar{b}_p^{m_1} = \bar{b}_p^{m_2}$. Since their two missing LSBs are copied from two adjacent quadrants of the *basic* Gray-coded QPSK, they will differ by one bit only. In conclusion, any two closest points of the obtained 2^{2p} -QAM constellation differ by only one bit and it is hence Gray-coded.

APPENDIX B

PROOF OF (25)

First, recall that $C_p = \tilde{C}_p \cup (-\tilde{C}_p) \cup \tilde{C}_p^* \cup (-\tilde{C}_p^*)$ and notice that each four symmetrical points ($\tilde{c}_m, \tilde{c}_m^*, -\tilde{c}_m$, and $-\tilde{c}_m^*$) have the same modulus. Therefore, one can rewrite (23) in an equivalent form by summing over \tilde{C}_p instead of C_p as follows:

$$D_\alpha(k) = \sum_{\tilde{c}_m \in \tilde{C}_p} e^{-\rho|\tilde{c}_m|^2} \times \left(\Pr[x(k) = \tilde{c}_m] \exp \left\{ \frac{\Re\{\tilde{c}_m y^*(k) S_{\phi,v}\}}{\sigma^2} \right\} + \Pr[x(k) = -\tilde{c}_m] \exp \left\{ \frac{\Re\{-\tilde{c}_m y^*(k) S_{\phi,v}\}}{\sigma^2} \right\} + \Pr[x(k) = \tilde{c}_m^*] \exp \left\{ \frac{\Re\{\tilde{c}_m^* y^*(k) S_{\phi,v}\}}{\sigma^2} \right\} + \Pr[x(k) = -\tilde{c}_m^*] \exp \left\{ \frac{\Re\{-\tilde{c}_m^* y^*(k) S_{\phi,v}\}}{\sigma^2} \right\} \right). \quad (87)$$

Now, after replacing the APPs involved in (87) by their explicit expressions already established in (16) to (19) and using the identity $e^x + e^{-x} = 2 \cosh(x)$, it can be shown that:

$$D_\alpha(k) = 2\beta_k \sum_{\tilde{c}_m \in \tilde{C}_p} \mu_{k,p}(\tilde{c}_m) e^{-\rho|\tilde{c}_m|^2} \times \left[\cosh \left(\frac{\Re\{\tilde{c}_m y^*(k) S_{\phi,v}\}}{\sigma^2} + \frac{L_{2p-1}(k)}{2} + \frac{L_{2p}(k)}{2} \right) + \cosh \left(\frac{\Re\{\tilde{c}_m^* y^*(k) S_{\phi,v}\}}{\sigma^2} + \frac{L_{2p-1}(k)}{2} - \frac{L_{2p}(k)}{2} \right) \right]. \quad (88)$$

Furthermore, by using the relationship $\cosh(x) + \cosh(y) = 2 \cosh\left(\frac{x+y}{2}\right) \cosh\left(\frac{x-y}{2}\right)$ along with the two identities $\tilde{c}_m + \tilde{c}_m^* = 2\Re\{\tilde{c}_m\}$ and $\tilde{c}_m - \tilde{c}_m^* = 2j\Im\{\tilde{c}_m\}$, it can be shown that (88) is rewritten as follows:

$$D_\alpha(k) = 4\beta_k \sum_{\tilde{c}_m \in \tilde{C}_p} \mu_{k,p}(\tilde{c}_m) e^{-\rho|\tilde{c}_m|^2} \times \left[\cosh \left(\frac{S\Re\{\tilde{c}_m\} u(k)}{\sigma^2} + \frac{L_{2p}(k)}{2} \right) \times \cosh \left(\frac{S\Im\{\tilde{c}_m\} v(k)}{\sigma^2} - \frac{L_{2p-1}(k)}{2} \right) \right]. \quad (89)$$

in which $u(k)$ and $v(k)$ are defined as:

$$u(k) \triangleq \Re\{y^*(k) e^{j(\phi+2\pi kv)}\}, \quad (90)$$

$$v(k) \triangleq \Im\{y^*(k) e^{j(\phi+2\pi kv)}\}. \quad (91)$$

APPENDIX C

PROOF OF LEMMA 1

For better illustration, the two bits $\bar{b}_{2p-2}^{(i,n)}$ and $\bar{b}_{2p-3}^{(i,n)}$ are highlighted in red color in Fig. 2. Recall that, for each symbol $c_m \in \tilde{C}_p$, these two bits are inherited from the corresponding symbol $c_{m'}$ (in the previous $2^{2(p-1)}$ -QAM). Actually, they are added in "step 3" during the recursive construction of the lower-order $2^{2(p-1)}$ -QAM since they are indeed the two LSBs for each $c_{m'}$. Thus, their values depend on the quadrant in which the symbol $c_{m'}$ lies (with respect to the x' - and y' -axes in Fig. 2) and on the specific choice of the *basic* QPSK. In our case, the *basic* QPSK constellation is shown in Fig. 1(c) and hence it follows that:

$$\bar{b}_{2p-2}^{(i,n)} = \begin{cases} 1 & \text{iff } \Re\{c_{m'}\} > 0 \\ 0 & \text{iff } \Re\{c_{m'}\} < 0 \end{cases} \quad (92)$$

$$\bar{b}_{2p-3}^{(i,n)} = \begin{cases} 1 & \text{iff } \Im\{c_{m'}\} > 0 \\ 0 & \text{iff } \Im\{c_{m'}\} < 0 \end{cases} \quad (93)$$

For better understanding of the results in (92) and (93), we refer the reader to Fig. 2. In this Appendix, we will show why $\bar{b}_{2p-2}^{(i,n)} = \lfloor \frac{i-1}{2^{p-2}} \rfloor$ only and $\bar{b}_{2p-3}^{(i,n)} = \lfloor \frac{n-1}{2^{p-2}} \rfloor$ can be shown in the same way. To begin with, it follows from (30) that:

$$\Re\{c_{m'}\} > 0 \iff (2i - 1 - 2^{p-1}) > 0 \quad (94)$$

$$\Re\{c_{m'}\} < 0 \iff (2i - 1 - 2^{p-1}) < 0. \quad (95)$$

We will show subsequently that we also have:

$$(2i - 1 - 2^{p-1}) > 0 \iff \left\lfloor \frac{i-1}{2^{p-2}} \right\rfloor = 1, \quad (96)$$

$$(2i - 1 - 2^{p-1}) < 0 \iff \left\lfloor \frac{i-1}{2^{p-2}} \right\rfloor = 0 \quad (97)$$

But before delving into details, notice that from (94) to (97) we have $\Re\{c_{m'}\} > 0 \iff \lfloor \frac{i-1}{2^{p-2}} \rfloor = 1$ and $\Re\{c_{m'}\} < 0 \iff \lfloor \frac{i-1}{2^{p-2}} \rfloor = 0$ which simply yields, in light of (92), the fact that $\bar{b}_{2^{p-2}}^{(i,n)} = \lfloor \frac{i-1}{2^{p-2}} \rfloor$. Now, due to space limitations, we will show the equivalence in the left-hand side of (96) only. Similar manipulations can be used to show the equivalence that appears in the right-hand side of the same equation.

- (\implies): On one hand, we have $2i - 1 - 2^{p-1} > 0 \implies i > 2^{p-2} + 1/2 > 2^{p-2}$. However, since we are comparing integers, this implies that $i \geq 2^{p-2} + 1 \implies i - 1 \geq 2^{p-2}$ and, therefore, we have (a): $\frac{i-1}{2^{p-2}} \geq 1$. On the other hand, we have $i \leq 2^{p-1} \implies i < 2^{p-1} + 1$ and, therefore, we have (b): $\frac{i-1}{2^{p-2}} < 2^{p-1}/2^{p-2} = 2$. Thus, using (a) and (b), we obtain $1 \leq \frac{i-1}{2^{p-2}} < 2 \implies \lfloor \frac{i-1}{2^{p-2}} \rfloor = 1$.
- (\impliedby): We have $\lfloor \frac{i-1}{2^{p-2}} \rfloor = 1 \implies (i-1)/2^{p-2} \geq 1$, which implies $i \geq 2^{p-2} + 1 \implies i > 2^{p-2} + 1/2$ and, therefore, $2i - 1 - 2^{p-1} > 0$, which completes the proof of (96).

APPENDIX D PROOF OF THEOREM 1

This theorem will be shown by mathematical induction for all $p \geq 2$. In fact, for $p = 2$ (i.e., 16-QAM) it is seen from (11) that $\mu_{k,2}(\tilde{c}_m)$ involves the two first MSBs only:

$$\begin{aligned} \mu_{k,2}(\tilde{c}_m) &= e^{(2\bar{b}_1^{(n)} - 1)\frac{L_1(k)}{2}} e^{(2\bar{b}_2^{(i)} - 1)\frac{L_2(k)}{2}} \\ &= \theta_{k,4}(i)\theta_{k,3}(n), \quad \forall \tilde{c}_m \in \tilde{\mathcal{C}}_2, \end{aligned} \quad (98)$$

where $\theta_{k,4}(i)$ and $\theta_{k,3}(n)$ are given by $\theta_{k,3}(n) = e^{(2\bar{b}_1^{(n)} - 1)\frac{L_1(k)}{2}}$ and $\theta_{k,4}(i) = e^{(2\bar{b}_2^{(i)} - 1)\frac{L_2(k)}{2}}$. These are indeed special cases (for $p = 2$) of (35). Thus, the theorem is trivially verified at order $p = 2$. Now, assume that (34) is true at order $p - 1, \forall p > 3$ (i.e., the $2^{2(p-1)}$ -QAM). At order p (i.e., the 2^{2p} -QAM), we have from (32):

$$\begin{aligned} \mu_{k,p}(\tilde{c}_m) &= \mu_{k,p-1}(\tilde{c}_{m'}) \exp \left\{ (2\bar{b}_{2^{p-3}}^{(i)} - 1) \frac{L_{2^{p-3}}(k)}{2} \right\} \\ &\quad \times \exp \left\{ (2\bar{b}_{2^{p-2}}^{(n)} - 1) \frac{L_{2^{p-2}}(k)}{2} \right\}, \end{aligned} \quad (99)$$

where $\mu_{k,p-1}(\tilde{c}_{m'})$ is defined over the $2^{2(p-1)}$ -QAM constellation for which the property is assumed to hold true thereby implying:

$$\mu_{k,p-1}(\tilde{c}_{m'}) = \theta_{k,2(p-1)}(i')\theta_{k,2(p-1)-1}(n'), \quad (100)$$

in which i' and n' define the coordinates of $\tilde{c}_{m'}$ in the $2^{2(p-1)}$ constellation according to $\tilde{c}_{m'} = (2i' - 1)d_p + j(2n' - 1)d_p$. The expressions of $\theta_{k,2(p-1)}(i')$ and $\theta_{k,2(p-1)-1}(n')$ are given from (35) by:

$$\theta_{k,2(p-1)}(i') = \prod_{l=1}^{p-2} e^{(2\bar{b}_{2^l}^{(i')} - 1)\frac{L_{2^l}(k)}{2}} \quad (101)$$

$$\theta_{k,2(p-1)-1}(n') = \prod_{l=1}^{p-2} e^{(2\bar{b}_{2^{l-1}}^{(n')} - 1)\frac{L_{2^{l-1}}(k)}{2}}. \quad (102)$$

Injecting (100) in (99) and rearranging the terms, one obtains:

$$\begin{aligned} \mu_{k,p}(\tilde{c}_m) &= \left[\theta_{k,2(p-1)}(i') e^{(2\bar{b}_{2^{p-2}}^{(i)} - 1)\frac{L_{2^{p-2}}(k)}{2}} \right] \\ &\quad \times \left[\theta_{k,2(p-1)-1}(n') e^{(2\bar{b}_{2^{p-3}}^{(n)} - 1)\frac{L_{2^{p-3}}(k)}{2}} \right]. \end{aligned} \quad (103)$$

Recall that $\tilde{c}_{m'}$ lies in the top-right quadrant, $\tilde{\mathcal{C}}_{p-1}$, of the previous $2^{2(p-1)}$ -QAM constellation whose CCS is defined by the x' - and y' -axes in Fig. 2. Recall also from the analysis between (29) and (31) that the symbols $\tilde{c}_{m'}$ and \tilde{c}_m have exactly the same $2p - 4$ MSBs, i.e., $\bar{b}_{2^l}^{(i')} = \bar{b}_{2^l}^{(i)}$ and $\bar{b}_{2^{l-1}}^{(n')} = \bar{b}_{2^{l-1}}^{(n)}$ for $l = 1, 2, \dots, p - 2$. Using these results in (101) and (102), it follows that:

$$\theta_{k,2(p-1)}(i') = \prod_{l=1}^{p-2} e^{(2\bar{b}_{2^l}^{(i)} - 1)\frac{L_{2^l}(k)}{2}} \quad (104)$$

$$\theta_{k,2(p-1)-1}(n') = \prod_{l=1}^{p-2} e^{(2\bar{b}_{2^{l-1}}^{(n)} - 1)\frac{L_{2^{l-1}}(k)}{2}}. \quad (105)$$

Hence, by making use of (104) and (105) along with (33), it follows that:

$$\begin{aligned} \theta_{k,2(p-1)}(i') e^{(2\bar{b}_{2^{p-2}}^{(i)} - 1)\frac{L_{2^{p-2}}(k)}{2}} &= \left(\prod_{l=1}^{p-2} e^{(2\bar{b}_{2^l}^{(i)} - 1)\frac{L_{2^l}(k)}{2}} \right) e^{(2\bar{b}_{2^{p-2}}^{(i)} - 1)\frac{L_{2^{p-2}}(k)}{2}} \\ &= \prod_{l=1}^{p-1} e^{(2\bar{b}_{2^l}^{(i)} - 1)\frac{L_{2^l}(k)}{2}} \\ &= \theta_{k,2p}(i), \end{aligned} \quad (106)$$

where the last equality follows immediately from the definition in (35). Using the same steps in (106), we show that:

$$\theta_{k,2(p-1)-1}(n') e^{(2\bar{b}_{2^{p-3}}^{(n)} - 1)\frac{L_{2^{p-3}}(k)}{2}} = \theta_{k,2p-1}(n). \quad (107)$$

Finally, using (106) and (107) in (103) leads to $\mu_{k,p}(\tilde{c}_m) = \theta_{k,2p}(i)\theta_{k,2p-1}(n)$ meaning that the property is also true at order p and therefore it is always true. This completes the proof of the first part in *Theorem 1*. The proof of its second part (recursive relations) follows immediately from (106) and (107).

In fact, by using $\theta_{k,2p}(i) = \theta_{k,2(p-1)}(i') e^{(2\bar{b}_{2^{p-2}}^{(i)} - 1)\frac{L_{2^{p-2}}(k)}{2}}$, (37) is a direct result of the fact that $i' = \lfloor \frac{2i-1-2^{p-1}+1}{2} \rfloor$ which is obtained from (30). The recursive relation in (38) is shown similarly by considering the counter n' and using (107).

APPENDIX E PROOF OF LEMMA 3

First, we denote $S_p = \sum_{n=1}^{2^{p-1}} \theta_{k,2p-1}(n)$ and we show by mathematical induction the following property:

$$S_p = 2^{p-1} \prod_{l=1}^{p-1} \cosh(L_{2^l-1}(k)/2). \quad (P) \quad (108)$$

At order $p = 2$, we have $S_2 = \theta_{k,3}(1) + \theta_{k,3}(2)$. Moreover, from (35), we have $\theta_{k,3}(1) = e^{(2\bar{b}_1^{(1)}-1)\frac{L_1(k)}{2}}$ and $\theta_{k,3}(2) = e^{(2\bar{b}_2^{(1)}-1)\frac{L_1(k)}{2}}$. However, by inspecting the top-right quadrant of the 16-QAM constellation in Fig. 1(c), it is seen that $\bar{b}_1^{(1)} = 0$ and $\bar{b}_2^{(1)} = 1$. Thus, $S_2 = e^{-\frac{L_1(k)}{2}} + e^{+\frac{L_1(k)}{2}} = 2\cosh(L_1(k)/2)$ and consequently property (P) is verified at order $p = 2$. Now, assume that (P) is verified at order $p - 1$, i.e.:

$$S_{p-1} = \sum_{n=1}^{2^{p-2}} \theta_{k,2p-3}(n) = 2^{p-2} \prod_{l=1}^{p-2} \cosh(L_{2l-1}(k)/2). \quad (109)$$

Then, owing to the recursive expression of $\theta_{k,2p-1}(n)$ in (38), we have at order p :

$$S_p = \sum_{n=1}^{2^{p-1}} \theta_{k,2p-1}(n) = \sum_{n=1}^{2^{p-1}} \theta_{k,2p-3} \left(\frac{|2n-1-2^{p-1}|+1}{2} \right) \times \exp \left\{ \left(2 \left\lfloor \frac{n-1}{2^{p-2}} \right\rfloor - 1 \right) \frac{L_{2p-3}(k)}{2} \right\}. \quad (110)$$

Due to the existence of the floor function, we divide the sum in (110) into two sums from $n = 1$ to 2^{p-2} and from $n = 2^{p-2} + 1$ to 2^{p-1} as follows:

$$S_p = \sum_{n=1}^{2^{p-2}} \theta_{k,2p-3} \left(\frac{|2n-1-2^{p-1}|+1}{2} \right) \times e^{\left(\left\lfloor \frac{n-1}{2^{p-2}} \right\rfloor - \frac{1}{2} \right) L_{2p-3}(k)} + \sum_{n=2^{p-2}+1}^{2^{p-1}} \theta_{k,2p-3} \left(\frac{|2n-1-2^{p-1}|+1}{2} \right) \times e^{\left(\left\lfloor \frac{n-1}{2^{p-2}} \right\rfloor - \frac{1}{2} \right) L_{2p-3}(k)}. \quad (111)$$

Now, in the first sum we have $1 \leq n \leq 2^{p-2}$ implying $0 \leq \frac{n-1}{2^{p-2}} \leq 1 - 1/2^{p-2}$ and hence $\left\lfloor \frac{n-1}{2^{p-2}} \right\rfloor = 0$. In the second sum, however, we have $2^{p-2} + 1 \leq n \leq 2^{p-1}$ implying $1 \leq \frac{n-1}{2^{p-2}} \leq 2 - 1/2^{p-2}$ and hence $\left\lfloor \frac{n-1}{2^{p-2}} \right\rfloor = 1$. Using these results in (111), it follows that

$$S_p = e^{-\frac{L_{2p-3}(k)}{2}} \sum_{n=1}^{2^{p-2}} \theta_{k,2p-3} \left((|2n-1-2^{p-1}|+1)/2 \right) + e^{\frac{L_{2p-3}(k)}{2}} \sum_{n=2^{p-2}+1}^{2^{p-1}} \theta_{k,2p-3} \left((|2n-1-2^{p-1}|+1)/2 \right). \quad (112)$$

Further, noticing that $(|2n-1-2^{p-1}|+1)/2$ is always an integer, the following simple substitution $m = (|2n-1-2^{p-1}|+1)/2$ reveals that the two sums in (112) are identical and they are equal to: Using (113), shown at the bottom of the page, in (112) and the fact that (P) is true at order $p - 1$, i.e., the expression of S_{p-1} in (109), we obtain:

$$S_p = 2 \cosh \left(\frac{L_{2p-3}(k)}{2} \right) S_{p-1} = 2 \cosh \left(\frac{L_{2p-3}(k)}{2} \right) 2^{p-2} \prod_{l=1}^{p-2} \cosh(L_{2l-1}(k)/2) = 2^{p-1} \prod_{l=1}^{p-1} \cosh(L_{2l-1}(k)/2), \quad (114)$$

which is exactly (108), i.e., property (P) holds as well at order p and, therefore, (108) is always true. Now, by recalling the expression of $\beta_{k,2p-1}$ in (47), we have:

$$2\beta_{k,2p-1} \cosh(L_{2p-1}(k)/2) \sum_{n=1}^{2^{p-1}} \theta_{k,2p-1}(n) = 2 \left(\frac{1}{2^p} \prod_{l=1}^p \frac{1}{\cosh \left(\frac{L_{2l-1}(k)}{2} \right)} \right) \times \left(2^{p-1} \prod_{l=1}^p \cosh \left(\frac{L_{2l-1}(k)}{2} \right) \right) = 1.$$

This completes the proof of *Lemma 3*.

APPENDIX F DETAILS ABOUT THE DERIVATION OF THE OTHER EXPECTATIONS

By integrating over the pdf of $u(k)$, we obtain:

$$\begin{aligned} & \mathbb{E} \left\{ u(k) \frac{F'_{2p,\alpha}(u(k))}{F_{2p,\alpha}(u(k))} \right\} \\ &= \int_{-\infty}^{\infty} u(k) \frac{F'_{2p,\alpha}(u(k))}{F_{2p,\alpha}(u(k))} p[u(k); \alpha] du(k) \\ &= \frac{2\beta_{k,2p}}{\sqrt{2\pi\sigma^2}} \int_{-\infty}^{\infty} u(k) F'_{2p,\alpha}(u(k)) e^{-u(k)^2/2\sigma^2} du(k), \quad (115) \end{aligned}$$

$$\sum_{n=1}^{2^{p-2}} \theta_{k,2p-3} \left((|2n-1-2^{p-1}|+1)/2 \right) = \sum_{n=2^{p-2}+1}^{2^{p-1}} \theta_{k,2p-3} \left((|2n-1-2^{p-1}|+1)/2 \right) = \sum_{m=1}^{2^{p-2}} \theta_{k,2p-3}(m) = S_{p-1} \quad (113)$$

in which the first derivative of the function $F_{2p,\alpha}(\cdot)$ defined in (41) is given by:

$$F'_{2p,\alpha}(x) = \frac{Sd_p}{\sigma^2} \sum_{i=1}^{2p-1} (2i-1)\theta_{k,2p}(i)e^{-\rho d_p^2(2i-1)^2} \times \sinh\left(\frac{(2i-1)d_p Sx}{\sigma^2} + \frac{L_{2p}(k)}{2}\right). \quad (116)$$

Plugging (116) in (115) and inverting the integral and sum signs, we obtain after some algebraic manipulations the following closed-form expression:

$$\begin{aligned} & \mathbb{E} \left\{ u(k) \frac{F'_{2p,\alpha}(u(k))}{F_{2p,\alpha}(u(k))} \right\} \\ &= \rho 4d_p^2 \beta_{k,2p} \cosh\left(\frac{L_{2p}(k)}{2}\right) \sum_{i=1}^{2p-1} (2i-1)^2 \theta_{k,2p}(i) \\ &= \rho \omega_{k,2p}, \end{aligned} \quad (117)$$

where $\omega_{k,2p}$ is defined in (56) for $r = 2p$. Likewise, we have:

$$\begin{aligned} \mathbb{E} \left\{ \frac{F''_{2p,\alpha}(u(k))}{F_{2p,\alpha}(u(k))} \right\} &= \int_{-\infty}^{\infty} \frac{F''_{2p,\alpha}(u(k))}{F_{2p,\alpha}(u(k))} p[u(k); \alpha] du(k) \\ &= \frac{2\beta_{k,2p}}{\sqrt{2\pi\sigma^2}} \int_{-\infty}^{\infty} F''_{2p,\alpha}(u(k)) e^{-\frac{u(k)^2}{2\sigma^2}} du(k). \end{aligned} \quad (118)$$

Starting from (116), we establish the second derivative of $F_{2p,\alpha}(\cdot)$ defined in (41) as follows:

$$F''_{2p,\alpha}(x) = \frac{S^2 d_p^2}{\sigma^4} \sum_{i=1}^{2p-1} (2i-1)^2 \theta_{k,2p}(i) e^{-\rho d_p^2(2i-1)^2} \times \cosh\left(\frac{(2i-1)d_p Sx}{\sigma^2} + \frac{L_{2p}(k)}{2}\right). \quad (119)$$

Then, plugging (119) in (118) and inverting the sum and integral signs, we express (118) in closed form as follows:

$$\begin{aligned} \mathbb{E} \left\{ \frac{F''_{2p,\alpha}(u(k))}{F_{2p,\alpha}(u(k))} \right\} &= 2\beta_{k,2p} \cosh\left(\frac{L_{2p}(k)}{2}\right) \\ &\quad \times \sum_{i=1}^{2p-1} \theta_{k,2p}(i) \frac{S^2 d_p^2 (2i-1)^2}{\sigma^4} \\ &= \frac{\omega_{k,2p}}{\sigma^2} \rho. \end{aligned} \quad (120)$$

Finally, we also have:

$$\begin{aligned} \mathbb{E} \left\{ \left(\frac{F'_{2p,\alpha}(u(k))}{F_{2p,\alpha}(u(k))} \right)^2 \right\} &= \int_{-\infty}^{\infty} \frac{F_{2p,\alpha}^2(u(k))}{F_{2p,\alpha}^2(u(k))} p[u(k); \alpha] du(k) \\ &= \frac{2\beta_{k,2p}}{\sqrt{2\pi\sigma^2}} \int_{-\infty}^{\infty} \frac{F_{2p,\alpha}^2(u(k))}{F_{2p,\alpha}(u(k))} \\ &\quad \times e^{-\frac{u(k)^2}{2\sigma^2}} du(k), \end{aligned}$$

which is simplified by changing $\frac{U(n)}{\sigma}$ by t and using $\rho = \frac{S^2}{2\sigma^2}$ to obtain (61).

ACKNOWLEDGMENT

The authors would like to thank the Associate Editor and all the anonymous reviewers for their constructive comments. In particular, one of them who has our deepest gratitude made us realize that the derived bounds also hold for LDPC-coded systems using turbo processing.

REFERENCES

- [1] "Technical specification group radio access network; Evolved universal terrestrial radio access (E-UTRA); Physical channels and modulation," Cedex, France, 3GPP TS 36.211, 2010.
- [2] C. Berrou and A. Glavieux, "Near optimum error correcting coding and decoding: Turbo codes," *IEEE Trans. Commun.*, vol. 44, no. 10, pp. 1261–1271, Oct. 1996.
- [3] S. L. Goff, A. Glavieux, and C. Berrou, "Turbo-codes and high spectral efficiency modulation," in *Proc. ICC*, New Orleans, LA, USA, May 1994, pp. 645–649.
- [4] C. Berrou, "The ten-year old turbo codes are entering into service," *IEEE J. Commun. Mag.*, vol. 41, no. 8, pp. 110–116, Aug. 2003.
- [5] *Part 16: Air Interface for Fixed and Mobile Broadband Wireless Access Systems-Amendment 2: Physical and Medium Access Control Layers for Combined Fixed and Mobile Operation in Licensed Bands*, IEEE Std 802.16e-2005, Feb. 2006.
- [6] 3rd Generation Partnership Project, (2007). Multiplexing and channel coding (FDD) (Release 8), Cedex, France, 3GPP TS 36.212 v8.0.0 (2007-09). [Online]. Available: <http://www.3gpp.org/Highlights/LTE/LTE.htm>
- [7] Y. Sun, Y. Zhu, M. Goel, and J. Cavallaro, "Configurable and scalable high throughput turbo decoder architecture for multiple 4G wireless standards," in *Proc. IEEE Int. Conf. Appl.-Specific Syst., Archit. Process.*, Leuven, Belgium, Jul. 2008, pp. 209–214.
- [8] A. Anastopoulos and K. M. Chugg, "Adaptive iterative detection for phase tracking in turbo-coded systems," *IEEE Trans. Commun.*, vol. 49, no. 12, pp. 2135–2144, Dec. 2001.
- [9] B. Mielczarek and A. Svensson, "Phase offset estimation using enhanced turbo decoders," in *Proc. IEEE Int. Conf. Commun.*, New York, NY, USA, Apr. 2002, vol. 3, pp. 1536–1540.
- [10] V. Lottici and M. Luise, "Embedding carrier phase recovery into iterative decoding of turbo-coded linear modulations," *IEEE Trans. Commun.*, vol. 52, no. 4, pp. 661–669, Apr. 2004.
- [11] K. Choi, "Residual frequency offset compensation-embedded turbo decoder," *IEEE Trans. Veh. Technol.*, vol. 57, no. 5, pp. 3211–3217, May 2008.
- [12] T. Ketsoglou and H. Wymeersch, "Optimized iterative (Turbo) reception for QAM OFDM with CFO over unknown double-selective channels," in *Proc. IEEE WTS*, New York, NY, USA, Apr. 2011, pp. 1–5.
- [13] N. Wiberg, "Simultaneous decoding and phase synchronization using iterative turbo decoding," in *Proc. IEEE Int. Symp. Inf. Theory*, Ulm, Germany, Jun. 29–Jul. 4, 1997, p. 11.
- [14] C. Kominakis and R. D. Wesel, "Joint iterative channel estimation and decoding in flat correlated rayleigh fading," *IEEE J. Sel. Areas Commun.*, vol. 19, no. 9, pp. 1706–1717, Sep. 2001.
- [15] C. Morlet, I. Buret, and M. L. Boucheret, "A carrier phase estimator for multi-media satellite payloads suited to RSC coding schemes," in *Proc. IEEE ICC*, New Orleans, LA, USA, Jun. 2000, vol. 1, pp. 455–459.
- [16] C. Langlais and M. Helard, "Phase carrier recovery for turbo codes over a satellite link with the help of tentative decisions," in *Proc. 2nd Int. Symp. Turbo Codes Related Topics*, Sep. 2000, vol. 5, pp. 439–442.
- [17] S. Cioni, G. E. Corazza, and A. Vanelli-Coralli, "Turbo embedded estimation with imperfect phase/frequency recovery," in *Proc. IEEE Int. Conf. Commun.*, Anchorage, AK, USA, Jun. 2003, pp. 2385–2389.
- [18] W. Oh and K. Cheun, "Joint decoding and carrier phase recovery algorithm for turbo codes," *IEEE Commun. Lett.*, vol. 5, no. 9, pp. 375–377, Sep. 2001.
- [19] N. Noels *et al.*, "Turbo-synchronization: An EM algorithm approach," in *Proc. IEEE Int. Conf. Commun.*, Anchorage, AK, USA, Jun. 2003, pp. 2933–2937.
- [20] X. Wu, Y. Song, C. Zhao, and X. You, "Progressive frequency offset compensation in turbo receivers," *IEEE Trans. Wireless Commun.*, vol. 10, no. 2, pp. 702–709, Feb. 2011.
- [21] C. Herzet, "Code-aided Synchronization for Digital Burst Communications," Ph.D. dissertation, Université Catholique de Louvain, Louvain, Belgium, 2006. [Online]. Available: http://dial.academielouvain.be/downloader/downloader.php?pid=boreal:5032&datastream=PDF_01

- [22] S. M. Kay, *Fundamentals of Statistical Signal Processing, 1: Estimation Theory*. Englewood Cliffs, NJ, USA: Prentice-Hall, 1998.
- [23] B. Cowley, F. Rice, and M. Rice, "Cramér-Rao lower bound for QAM phase and frequency estimation," *IEEE Trans. Commun.*, vol. 49, no. 9, pp. 689–693, Sep. 2001.
- [24] F. Gini, R. Reggiannini, and U. Mengali, "The modified Cramér-Rao bound in vector parameter estimation," *IEEE Trans. Commun.*, vol. 46, no. 1, pp. 52–60, Jan. 1998.
- [25] J. P. Delmas, "Closed form-expressions of the exact Cramér-Rao bound for parameter estimation of BPSK, MSK, or QPSK waveforms," *IEEE Signal Process. Lett.*, vol. 15, pp. 405–408, 2008.
- [26] F. Bellili, N. Atallah, S. Affes, and A. Stéphenne, "Cramér-Rao lower bounds for frequency and phase NDA estimation from arbitrary square QAM-modulated signals," *IEEE Trans. Signal Process.*, vol. 58, no. 9, pp. 4517–4525, Sep. 2010.
- [27] F. Bellili, A. Stéphenne, and S. Affes, "Cramér-Rao bounds for NDA SNR estimates of square QAM modulated signals," in *Proc. IEEE WCNC*, Budapest, Hungary, Apr. 2009, pp. 1–5.
- [28] F. Bellili, A. Stéphenne, and S. Affes, "Cramér-Rao lower bounds for NDA SNR estimates of square QAM modulated transmissions," *IEEE Trans. Commun.*, vol. 58, no. 11, pp. 3211–3218, Nov. 2010.
- [29] F. Bellili, S. B. Hassen, S. Affes, and A. Stéphenne, "Cramer-rao lower bounds of DOA estimates from square QAM-modulated signals," *IEEE Trans. Commun.*, vol. 59, no. 6, pp. 1675–1685, Jun. 2011.
- [30] A. Masmoudi, F. Bellili, S. Affes, and A. Stéphenne, "Closed-form expressions for the exact Cramér-Rao bounds of timing recovery estimators from BPSK, MSK and square-QAM transmissions," *IEEE Trans. Signal Process.*, vol. 59, no. 6, pp. 2474–2484, Jun. 2011.
- [31] A. Masmoudi, F. Bellili, S. Affes, and A. Stéphenne, "Closed-form expressions for the exact Cramer-Rao bounds of timing recovery estimators from BPSK and square-QAM transmissions," in *Proc. IEEE Int. Conf. Commun.*, Kyoto, Japan, Jun. 2011, pp. 1–6.
- [32] L. Bahl, J. Cocke, F. Jelinek, and J. Raviv, "Optimal decoding of linear codes for minimizing symbol error rate," *IEEE Trans. Inf. Theory*, vol. IT-20, no. 2, pp. 284–287, Mar. 1974.
- [33] N. Noels, H. Steendam, and M. Moeneclaey, "Carrier and clock recovery in (turbo) coded systems: Cramér-Rao bound and synchronizer performance," *EURASIP J. Appl. Signal Process., Spec. Issue Turbo Process.*, vol. 2005, no. 6, pp. 972–980, May 2005.
- [34] J. A. C. Bingham, "Multicarrier modulation for data transmission: An idea whose time has come," *IEEE Commun. Mag.*, vol. 28, no. 5, pp. 5–14, May 1990.
- [35] Z. Wang and G. B. Giannakis, "Wireless multicarrier communications: Where Fourier meets Shannon," *IEEE Signal Process. Mag.*, vol. 17, no. 3, pp. 29–48, May 2000.
- [36] N. Noels, H. Steendam, and M. Moeneclaey, "The Cramér-Rao bound for phase estimation from coded linearly modulated signals," *IEEE Commun. Lett.*, vol. 7, no. 5, pp. 207–209, May 2003.
- [37] U. Mengali and A. N. D'Andrea, *Synchronization Techniques for Digital Receivers*. New York, NY, USA: Plenum, 1997.
- [38] M. M. Mansour and N. R. Shanbhag, "High throughput LDPC decoders," *IEEE Trans. Very Large Scale Integr. (VLSI) Syst.*, vol. 11, no. 6, pp. 976–996, Dec. 2003.
- [39] G. Gentile, M. Rovini, and L. Fanucci, "A multi-standard flexible turbo/LDPC decoder via ASIC design," in *Proc. Int. Symp. Turbo Codes Iterative Inf. Process.*, 2010, pp. 294–298.
- [40] G. Colavolpe, G. Ferrari, and R. Raheli, "Extrinsic information in iterative decoding: A unified view," *IEEE Trans. Commun.*, vol. 49, no. 12, pp. 2088–2094, Dec. 2001.
- [41] S. Y. Le Goff, B. K. Khoo, and C. C. Tsimenidis, "Constellation shaping for bandwidth-efficient turbo-coded modulation with iterative receiver," *IEEE Trans. Wireless Commun.*, vol. 6, no. 6, pp. 2223–2233, Jun. 2007.
- [42] C. Herzet *et al.*, "Code-aided turbo synchronization," *Proc. IEEE*, vol. 95, no. 6, pp. 1255–1271, Jun. 2007.
- [43] A. N. D'Andrea, U. Mengali, and R. Reggiannini, "The modified Cramér-Rao bound and its application to synchronization parameters," *IEEE J. Sel. Areas Commun.*, vol. 42, no. 2–4, pp. 1391–1399, Apr. 1994.



Faouzi Bellili was born in Tunisia, on June 16, 1983. He received the B.Eng. degree (with Hons.) in signals and systems from the Tunisia Polytechnic School in June 2007, and the M.Sc. and Ph.D. degrees (both with the highest honor) from the National Institute of Scientific Research (INRS-EMT), University of Quebec, Montreal, QC, Canada, in December 2009 and August 2014, respectively. He is currently working as a Research Associate at the INRS-EMT. He authored/co-authored over 40 peer-reviewed papers in reputable IEEE journals and conferences. His research focuses on statistical signal processing and array processing with an emphasis on parameters estimation for wireless communications. He was selected by the INRS as its candidate for the 2009–2010 competition of the very prestigious Vanier Canada Graduate Scholarships program. He also received the Academic Gold Medal of the Governor General of Canada for the year 2009–2010 and the Excellence Grant of the Director General of INRS for the year 2009–2010. He also received the award of the best M.Sc. thesis of INRS-EMT for the year 2009–2010 and twice—for both the M.Sc. and Ph.D. programs—the National Grant of Excellence from the Tunisian Government. He was rewarded in 2011 the Merit Scholarship for Foreign Students from the Ministère de l'Éducation, du Loisir et du Sport (MELS) of Québec, Canada. He serves as a TPC member for the IEEE GLOBECOM conference and he acts regularly as a reviewer for many international scientific journals and conferences.



Achref Methenni was born in Dammam, Saudi Arabia, on November 19, 1987. He received the Diplôme d'Ingénieur degree in telecommunication from the Ecole Supérieure des Communications de Tunis-Sup'Com (Higher School of Communication of Tunis), Tunisia, in 2011 and the M.Sc. degree from the Institut National de la Recherche Scientifique-Energie, Matériaux, et Télécommunications (INRS-EMT), Université du Québec, Montréal, QC, Canada, in 2013. He is currently working toward the Ph.D. degree at INRS, Montreal, QC, Canada.

His research activities include signal processing for Turbo-coded systems, and parameters estimation for wireless communications in general. He received twice—for both the M.Sc. and Ph.D. programs—the National Grant of Excellence from the Tunisian Government.



Sofiene Affes (SM'04) received the Diplôme d'Ingénieur in telecommunications in 1992, and the Ph.D. degree with honors in signal processing in 1995, both from École Nationale Supérieure des Télécommunications (ENST), Paris, France. He has since been with INRS, Canada, as a Research Associate until 1997, an Assistant Professor until 2000, and Associate Professor until 2009. Currently, he is Full Professor and Director of PERSWADE, a unique \$4M research training program on wireless in Canada involving 27 faculty from eight universities

and ten industrial partners. He has been twice the recipient of a Discovery Accelerator Supplement Award from NSERC, from 2008 to 2011, and from 2013 to 2016. From 2003 to 2013, he held a Canada Research Chair in Wireless Communications. In 2006, he served as General Co-Chair of IEEE VTC'2006-Fall, Montreal, Canada. In 2008, he received from the IEEE Vehicular Technology Society the IEEE VTC Chair Recognition Award for exemplary contributions to the success of IEEE VTC. He currently acts as an Associate Editor for the IEEE TRANSACTIONS ON COMMUNICATIONS and the Wiley Journal on Wireless Communications & Mobile Computing. From 2007 until 2013 and from 2010 until 2014, he was an Associate Editor for the IEEE TRANSACTIONS ON WIRELESS COMMUNICATIONS and the IEEE TRANSACTIONS ON SIGNAL PROCESSING, respectively. He is serving now as General Co-Chair of IEEE ICUBW to be held in Montreal in the fall 2015.